Behavioral circatidal rhythms require Bmal1 in Parhyale hawaiensis

Authors: Erica R. Kwiatkowski[1], Yisrael Schnytzer[2.3], Joshua J.C. Rosenthal[3] and Patrick Emery[1,4, 5,*]

[1] Department of Neurobiology, University of Massachusetts Chan Medical School, Worcester, MA 01605, USA
[2] The Leslie and Susan Gonda Multidisciplinary Brain Research Center, Bar-Ilan University, Ramat Gan, 5290002, Israel
[3] The Eugene Bell Center, The Marine Biological Laboratory, Woods Hole, MA 02543, USA
[4] Twitter: @LabEmery
[5] Lead Contact

* Correspondence: Patrick.Emery@umassmed.edu. Tel: 508-856-6599

Summary

Organisms living in the intertidal zone are exposed to a particularly challenging environment. In addition to daily changes in light intensity and seasonal changes in photoperiod and weather patterns, they experience dramatic oscillations in environmental conditions due to the tides. To anticipate tides, and thus optimize their behavior and physiology, animals occupying intertidal ecological niches have acquired circatidal clocks. While the existence of these clocks has long been known, their underlying molecular components have proven difficult to identify, in large part because of the lack of an intertidal model organism amenable to genetic manipulation. In particular, the relationship between the circatidal and circadian molecular clocks, and the possibility of shared genetic components, has been a long-standing question. Here, we introduce the genetically-tractable crustacean *Parhyale hawaiensis* as a system for the study of circatidal rhythms. First, we show that *P. hawaiensis* exhibits robust 12.4-h rhythms of locomotion that can be entrained to an artificial tidal regimen and are temperature-compensated. Using CRISPR/Cas9-genome editing, we then demonstrate that the core circadian clock gene *Bmal1* is required for circatidal rhythms. Our results thus demonstrate that *Bmal1* is a molecular link between circatidal and circadian clocks and establish *P. hawaiensis* as a powerful system to study the molecular mechanisms underlying circatidal rhythms and their entrainment.

Introduction

Biological clocks are critical for organisms to optimize their physiology and behavior to environmental cycles. Among them, circadian clocks are by far the best understood. Starting with the identification of the first core circadian clock gene (*period* [*per*]) in 1971 [1] and its molecular characterization in 1984 [2-4], a remarkably detailed understanding of circadian rhythms, and their impact on organismal physiology, has emerged [5,6]. Biological rhythms entrained by environmental cycles of different periods, however, have received less scientific attention. Circatidal rhythms - those entrained by the rhythmic rising and falling of the tides - are an intriguing and understudied example.

Tides are generated by the gravitational pull of the Moon as it rotates around the Earth, and the centrifugal force generated by this system [7,8]. In most coastal locations, this produces tides with a period of 12.4 hours (h) (semi-diurnal tides), half of the 24.8 h it takes for the Earth to rotate until the Moon has returned to its same position in the sky. Circatidal rhythms of behavior were first observed in the Roscoff worm (*Convoluta roscoffensis*) more than 100 years ago [8-10]. Experiments during the 1950's on the fiddler crab, *Uca pugnax*, and the mussel, *Mytilus californianus*, further demonstrated robust circatidal rhythms of activity that supported the existence of an autonomous circatidal pacemaker [11,12]. However, the molecular nature of that pacemaker, and its relationship to the circadian pacemaker (including the possibility of a shared identity), have been enduring questions. Three competing models have been proposed [13-15]. Enright hypothesized that a single bimodal clock generates both circadian and circatidal rhythmicities [15]. In contrast, Naylor proposed that circatidal behavioral rhythms are the result of a distinct tidal clock, running at 12.4 h, that can be modulated by a circadian clock running at 24 h [16,17]. Palmer and Williams, however, presented a model in which paired circalunidian clocks, each running at 24.8 h, operate in opposite phases to produce 12.4 h rhythms [18]. Interestingly, the circadian molecular clock utilizes a pair of interlocked feedback loops to drive rhythms of gene expression 12 h apart [19-21], and could provide such a mechanism with a slight adjustment of period. Moreover, plasticity in circadian period and circadian clock gene expression patterns in response to envrionmental conditions have been observed in marine worms and oysters, respectively [22-24].

Knockdown of circadian gene expression by RNA interference (RNAi) was used in the intertidal organisms *Apteronemobius asahinai* and *Eurydice pulchra* to determine whether the two clocks shared components. Circatidal behavior appeared to be unaffected, suggesting that the core circadian genes *period (per)* and *Clock* (*Clk*) are not involved in the generation of circatidal behavioral rhythms [25-27]. However, pharmacological inhibition of CKIδ/ε, which regulates circadian rhythms in flies and mammals [28-30], altered circatidal period in *E. pulchra*, thus raising the possibility that some elements of the circadian clock might also play a role in circatidal rhythms [25]. Importantly, dsRNA injection in *E. pulchra* and *A. asahinai* only partially suppressed circadian gene expression, leaving the possibility that the remaining gene expression was sufficient to drive the circatidal clock. Thus, a circatidal model organism that can be manipulated to produce complete and specific genetic knock-outs would be critical to determine conclusively if circadian genes are required for the generation of circatidal rhythms and to identify genes specific to the circatidal clock.

Parhyale hawaiensis is a small amphipod crustacean easily propagated in the lab. Its genome is fully sequenced, and it is amenable to CRISPR/Cas9-guided genome editing and transgenesis [31-33]. *P. hawaiensis* lives in tropical regions around the world, residing in shallow waters within the upper intertidal zone, and is thus subjected to constant tidal cycles [31,34,35]. Accordingly, it would appear to be an ideal candidate for examining the molecular underpinnings of circatidal behaviors through genetic manipulations. However, whether *P. hawaiensis* displays circatidal rhythms has yet to be established.

Circadian clock gene homologs have been identified in the genome of *P. hawaiensis* [36], and its circadian clock appears to be similar to that of mammals, although this has not been tested experimentally. The proposed model of the *P. hawaiensis* circadian clock predicts that the transcriptional activator PhCLK and PhBMAL1 interact to promote expression of two transcriptional repressors, PhPER and PhCRYPTOCHROME2 (PhCRY2) [36]. PhPER and PhCRY2 presumably repress their own transcription, as demonstrated in mammals and other species [37-40]. With these genetic features, establishing a method to observe and entrain circatidal behavior in *P.*

hawaiensis would allow to test rigorously whether circadian genes are also involved in the circatidal clock.

Here, we report that *P. hawaiensis* exhibits circatidal swimming behavior in constant conditions after entrainment to an artificial tidal regimen. We show that CRISPR-Cas9 mediated mutagenesis of the circadian clock gene *PhBmal1* disrupts both circadian and circatidal rhythms, demonstrating that the mechanisms underlying circatidal and circadian rhythms are controlled by at least one common factor. By reporting the first engineered circatidal mutant, we establish *P. hawaiensis* as a promising, genetically-tractable model organism for the elucidation of the mechanisms underlying circatidal rhythms.

Results

Parhyale hawaiensis exhibits rhythmic swimming activity after tidal entrainment

P. hawaiensis is distributed around the globe in the intertidal zones of tropical latitudes [31]. We therefore expected it would possess a circatidal clock capable of driving rhythmic swimming behavior. We thus created artificial semidiurnal tidal cycles simulating the tides experienced by a shallow-water dweller like *P. hawaiensis*, using water tanks that were filled and emptied by timed pumps (Figure 1A). During the 10.25-h high tide, animals were submerged in ~5 cm of artificial sea water (ASW), while during the 2.15-h low tide all ASW was drained. Animals were concurrently exposed to a 12h light/12h dark (LD) cycle, and temperature was kept constant at 25ºC (Figure 1B). This entrainment protocol will be referred to as tidal entrainment while LD entrainment will refer to the entrainment regimen with only a LD cycle.

After exposing the animals to ten artificial semidiurnal tidal cycles, concurrent with a little more than five circadian light cycles, we moved them into constant darkness (DD) to examine their free-running behavior. Individual male *P. hawaiensis* were taken from the tidal tank and placed into a clear plastic tube with ~5cm of ASW, keeping the animals constantly at high tide (Figure 1C). These tubes were then placed in *Drosophila* Population Monitors (DPMs) oriented vertically, allowing activity to be recorded from two of the three infrared beam arrays (Figure 1C). Activity that triggered the middle array was termed “vertical swimming.”, while activity triggering the bottom array was termed “roaming”, since it only required the animal to move horizontally or a short distance vertically.

P. hawaiensis showed robustly rhythmic activity following tidal entrainment in DD, with about 73% of animals exhibiting rhythms of vertical swimming and 62.5% exhibiting rhythms of roaming, or 80% of animals exhibiting either vertical or roaming swimming rhythms (Figure 1D-O). Interestingly, activity levels showed strong peaks during the middle of the subjective (expected) high tides, and troughs coinciding with the subjective low tides (Figure 1D,F, H-J). Comparison of average rhythmic activity traces

for vertical swimming and roaming showed that both traces overlap well, with similar timing of activity peaks and troughs (Figure 1J). Although most rhythmic *P. hawaiensis* exhibited significant periods on both levels, a smaller group only had statistically significant vertical swimming rhythms, and very few only had statistically significant roaming rhythms (Figure 1N). However, neither the average period values nor the rhythmicity significantly differed between vertical swimming and roaming (1K-M). In the experiments described below, when an animal was rhythmic for both vertical swimming and roaming, we used the period of the most robust rhythm (based on power, see Methods) to calculate period averages.

As expected for circatidal rhythms [41], most rhythmic animals had statistically significant behavioral periodicities clustered around 12.4 h ("singlet") (Figure 1L) and 24.8 h ("doublet" harmonic) (Figure 1M) under constant high tide and DD conditions (Figure 1E,G). A small subset of rhythmic animals had only a significant singlet or doublet periodicity (Figure 1O). On closer examination, these were often animals with weaker rhythms, such that only one of the two periods reached significance (Figure S1). This explains why the number of animals may differ between the singlet and doublet averages. Periodograms also frequently identified a triplet period, which will not be discussed as this harmonic of 12.4 h was only observed along with shorter periodicities.

P. hawaiensis swimming rhythms are circatidal and entrained by artificial tides

Although both the average period and the behavior traces are consistent with entrainment to artificial semidiurnal tidal cycles, we wanted to rule out the possibility that the observed rhythmic behaviors were circadian behaviors, which were detected in a previous study wherein *P. hawaiensis* animals were exposed to a LD cycle, but not to artificial tides [42]. We thus first altered free-running conditions from DD to constant light (LL). Indeed, light is the major synchronizing cue for circadian clocks, and LL conditions usually disrupt circadian behavioral rhythms in animals, altering period length or causing arrhythmicity [43,44]. By contrast, circatidal clocks cannot utilize light as a synchronizing

cue since tides are not anchored to diurnal solar cycles, and should thus be largely insensitive to LL, as observed in *E. pulchra* [25].

P. hawaiensis exposed to artificial tides and LD cycles exhibited rhythmic behavior under LL that was similar to that of animals free-running in DD (Figure 2A-D). In particular, periods of singlets and doublets under LL exhibited virtually identical periods to those observed in DD (Figure 2F,G, Table S1). We noticed a non-significant reduction in rhythmicity (Figure 2E). Indeed, rhythmic vertical swimming behavior showed some changes from LL to DD. Its amplitude increased in LL, with sharper activity peaks and longer, lower activity troughs. However, the number of animals exhibiting vertical swimming rhythms decreased, with almost half of the rhythmic population only exhibiting rhythms of roaming activity (Figure 2H). This loss of vertical swimming rhythms might be adaptive in the wild, as animals might want to limit swimming under bright light, when they would be more at risk of predation. The increase in amplitude could also be a result of this, with deeper activity troughs and briefer periods of activity. We also noted that more animals exhibited only one (singlet or doublet) period value (Figure 2I). When comparing males and females under LL, we found males to be more rhythmic than females (Figure S2). However, there was no significant difference in the power of vertical swimming or roaming rhythms between rhythmic female and male animals (Figure S2). The lower percentage of rhythmicity in females might perhaps be due to their reproductive cycle, as females carry embryos in their ventral brood pouch for approximately two weeks [31]. In mice and humans, changes in activity level are observed during gestation [45]. Thus, only males were used for the rest of the study.

The 12.4 h period of swimming rhythms and their persistence in LL is consistent with a circatidal rhythm, rather than a circadian rhythm [25]. To confirm that these rhythms are indeed of circatidal nature, we determined whether they were entrained by the LD cycle or by the artificial tides. We delayed the phase of the artificial tides relative to the circadian cycle by six hours. Instead of the last high tide (LHT) on the last day of entrainment occurring at 13:20 (LHT 13:20), it occurred at 19:20 (LHT 19:20).

Importantly, we still moved the animals at the same time in the LD cycle, to avoid any confounding circadian time-dependent effects of animal manipulation.

Animals successfully entrained to the phase-shifted LHT 19:20 tidal cycle and exhibited circatidal rhythms of activity in both LL and DD conditions (Figure 2J,K, Figure S3). Comparison of the two regimens showed clear opposition of the peaks of activity, consistent with entrainment to two cycles set 6 h apart (Figure 2L,M, Figure S3). Notably, period values from animals entrained to LHT 13:20 and LHT 19:20 were almost identical (Table S1), and neither singlet period nor rhythmicity significantly differed between 13:20 and 19:20 LHT entrained animals (Figure 2N-P). *P. hawaiensis'* swimming rhythms are therefore entrained by the artificial tides and not the LD cycle, and are thus circatidal in nature.

P. hawaiensis exhibits distinct rhythmic swimming behavior after LD entrainment

As mentioned above, apparent circadian behavior was observed in *P. hawaiensis* when these animals were entrained only to a LD cycle, without artificial tides [42]. To determine whether these rhythms are distinct from the rhythms observed after tidal entrainment, we tested animals kept in a "circadian tank" exposed only to 12:12 LD cycles. Initial attempts to use the same approach as the tidally-entrained animals proved difficult, as only a very low proportion of animals displayed weak rhythms after LD entrainment in the tank. Thus, we exposed individual *P. hawaiensis* to an additional two LD cycles after transferring the animals to behavior recording tubes, before exposing them to DD.

With this approach, we observed markedly different activity patterns than those of tidal-entrained animals, with the most prominent peak occurring around 20:00 or Circadian Time (CT) 12, around the expected transition from light to dark, and shallow troughs of activity during the expected light period (Figure 3A,B). Out of 32 animals, 21 (65.6%) were rhythmic, and their average period was slightly, but significantly shorter than that of the tidally-entrained individuals (Figure 3C-E, Table S1). Notably, the fraction of animals exhibiting a singlet period value was reduced in animals entrained to LD only,

compared to tidal-entrained animals (39% vs. 84%) (Figure 3O). In addition, the average power of both vertical swimming and roaming rhythms after LD entrainment was significantly reduced compared to the averages observed after tidal entrainment (Figure 3F,G).

As expected for circadian rhythms [43,44] and in sharp contrast with the rhythms observed after tidal entrainment, constant light affected free-running rhythms after LD entrainment. The doublet period was about 1.3 h longer on average and much more variable under LL than under DD (Figure 3K,N). This increase in period under LL conditions would be expected for a circadian nocturnal animal under Aschoff's rule [46]. The fraction of animals exhibiting a singlet period was further reduced in LL compared to DD (8% vs. 39%) (Figure 3O). Curiously, vertical swimming and roaming rhythms were markedly stronger in LL, with an increased amplitude and a significant increase in average power of roaming rhythms (Figure 3H,I,M, S4). This is somewhat surprising, given that *P. hawaiensis'* circadian behavior is nocturnal. Average power of vertical swimming rhythms, as well as percent rhythmicity, did not significantly differ (Figure 3J,L).

In summary, our results establish that *P. hawaiensis* exhibits free-running circatidal rhythms distinct from circadian rhythms: their period closely matches that of tidal cycles, they are largely insensitive to light, and most importantly, they are entrained by tidal cycles. Interestingly, if only an LD cycle is present, *P. hawaiensis* can entrain and exhibit circadian behavior as well, suggesting behavioral flexibility to environmental conditions.

P. hawaiensis circatidal rhythms exhibit temperature compensation

Bona-fide circatidal rhythms should be entrained by tides, exhibit a ~12.4h periodicity, and be temperature-compensated [25]. To determine if the rhythms we observed also met this third criterion, we altered the ambient temperature during free-running (LL) conditions. The free-running behavior of animals at 19.5^{o}C and 30^{o}C displayed the

same pattern of activity relative to the expected tidal cycle, although rhythmic behavior at 19.5ºC seemed to show a faster decay (Figure 4A-D), and percentage of rhythmicity was reduced (Figure 4G). This may be because 19.5ºC is below the normal temperature range for this tropical species, and may generate stress responses [31]. Overlaying the average rhythmic trace from each temperature shows that the timing of activity peaks and troughs is consistent across all three temperatures (Figure 4E,F). Additionally, we observed a slight but significant decrease in the singlet period value between 19.5ºC and 30ºC, though not in the doublet period values (Figure 4H,I, Table S1). However, even for the singlets, the Q_{10} coefficient was well within the accepted range for a temperature-compensated biological rhythm (1.024, Figure 4H) [47].

Generating *PhBmal1*-mutant animals

The molecular mechanism underlying circatidal rhythms is unknown, but it has been proposed that it could utilize a similar mechanism to the circadian clock, perhaps even using some, if not most, of the same elements to generate 12.4 or 24.8 h oscillations in gene expression [48]. To determine whether the circadian and circatidal clocks share molecular components, we targeted the core circadian protein PhBMAL1. PhBMAL1, like most other BMAL1 proteins, contains a basic-helix-loop-helix (bHLH) domain, followed by two Per-Arnt-Sim (PAS) domains, and a BMAL1 C-terminal region BCTR [36] (Figure 5E). The BCTR domain has been shown to be required for transcriptional activation and free-running behavioral and molecular rhythms in constant conditions in mice and numerous invertebrates, including crustaceans [25,49-54]. The transactivation domain (TAD) contained within the BCTR is also required for both mammalian CRY1 and 2 to bind and is thus needed for transcriptional repression [50,55,56]. Thus, these two domains are required for activity.

To generate a mutant *PhBmal1* allele with reduced or no activity, two gRNAs were designed that target nearby sequences within the PAS-B domain (Figure 5A, B). Both were co-injected with Cas9 enzyme into *P. hawaiensis* embryos. Colonies were established and animals were tested for mutations by PCR. Gel electrophoresis

revealed fragments of three different sizes in one colony, indicating the presence of a mutant allele (Figure 5D). Sequencing of the smaller PCR product revealed two small deletions at each gRNA site, causing in sum a 16nt deletion and thus generating a frame shift and a premature stop codon that truncates the PAS-B domain and eliminates the BCTR (Figure 5C,E,F). The intermediate band corresponded to the wild-type allele. Sequencing of the slow-migrating band observed only in heterozygote animals revealed a hybrid product of wild-type and mutant sequences. Its slower gel migration is presumably the result of the presence of two unpaired DNA loops caused by the deletions, a well-known phenomenon [57,58].

We used a transcriptional assay in Human Embryonic Kidney (HEK) 293 cells to verify that the mutant *Bmal1* allele (referred to as *PhBmal1*$^{\Delta}$) encodes for a defective protein, as predicted [25,49-55]. We co-expressed wild-type or mutant PhBMAL1, along with mouse (m)CLK, in HEK293 cells in the presence of a Luciferase reporter plasmid driven by multiple E-boxes. We chose to evaluate PhBMAL1's ability to transactivate in the presence of mCLK rather than PhCLK because the latter's published sequence is missing the region encoding the PAS-B domain and the polyglutamine region characteristic of this protein, and might thus be incomplete [36]. As expected, mBMAL1 was able to associate with mCLK to activate Luciferase expression (Figure 5G). Interestingly, wild-type PhBMAL1 was also able to activate luciferase transcription with mCLK. However, PhBMAL1$^{\Delta}$ did not, and this lack of activity was not caused by differences in protein levels (Figure 5G-I). PhBMAL1$^{\Delta}$ is therefore a severely defective protein.

These transactivation experiments strongly indicate that the *PhBmal1*$^{\Delta}$ allele is amorphic. Furthermore, when testing swimming rhythms after LD entrainment, we observed severely disrupted circadian behavior. When animals were allowed to free-run in DD, shallow rhythms were observed in wild-type and heterozygous animals (Figure 6A,B; S5A,B). For unknown reasons, rhythms were weaker in wild-type homozygotes than those observed with the wild-types from the parent colony, but *PhBmal1*$^{+/\Delta}$ heterozygotes showed comparable rhythms (Figure 3A-C and 6A,B,

S5A,B). On the other hand, no obvious rhythms could be observed on the average behavior trace of *PhBmal1*$^{\Delta/\Delta}$ animals (Figure 6C, S5C). Although about 30% of individual mutants were still statistically significantly rhythmic, they did not seem to anticipate subjective light or dark periods and the average power of roaming was significantly decreased in homozygous mutants compared to wild-type controls (Figure 6D,E, S5I). Importantly, the periods from these rhythms did not cluster around 12 or 24 h as in wild-type and heterozygote animals, but instead showed striking variability (Figure 6F).

Since we had observed more robust rhythms with the wild-type parent colony under LL than under DD (Figure 3 and S4), we also tested LD-entrained animals from the *PhBmal1*$^{\Delta}$ colony in LL. Homozygous wild-type animals exhibited stronger and more robust circadian rhythms with a longer period under LL, comparable to those seen in the parent colony (Figure 6G, S6A). Rhythmicity was however reduced in *PhBmal1*$^{\Delta/+}$ animals, presumably because their oscillator is weakened by the loss of a functional allele (Figure 6H, S6B). Indeed, weakened circadian oscillators are more sensitive to environmental inputs [59,60]. Importantly, circadian rhythms were severely disrupted in *PhBmal1*$^{\Delta/\Delta}$ mutants. No discernable rhythm was observed on the average behavioral trace (Figure 6I, S6C). Only 22% of mutant animals were rhythmic, in striking contrast with the homozygous controls (68%). Power for these few rhythmic mutant animals was very low (Figure 6J,K), and as observed in DD, period distribution was abnormal (Figure 6L, S6D-G). We therefore conclude that loss of PhBMAL1 severely disrupts circadian rhythms in *P. hawaiensis*, leaving only residual rhythms of poorly defined periods.

PhBmal1 is required for behavioral circatidal rhythms in *P. hawaiensis*

We then tested whether *PhBmal1*$^{\Delta/\Delta}$ mutant animals expressed circatidal rhythms. Compared to *PhBmal1*$^{+/+}$ and *PhBmal1*$^{+/\Delta}$ animals, *PhBmal1*$^{\Delta/\Delta}$ animals exhibited striking deficits in circatidal behavior. The average activity traces of wild-type and heterozygous animals closely resembled that of wild-type animals in previous experiments (Figure 7A-D), but *PhBmal1*$^{\Delta/\Delta}$ traces were arrhythmic, with just one peak

of activity detectable on the first day of constant conditions (Figure 7E,F). Percent rhythmicity was indeed severely reduced in mutant animals compared to both wild-type and heterozygous animals (Figure 7N).

Additionally, the periods measured from rhythmic *PhBmal1*$^{\Delta/\Delta}$ provided further evidence of severe disruption to the free-running circatidal swimming rhythms. Wild-type and heterozygous animals showed the expected circatidal period of ca. 12.4 h or 24.8 h. However, for the few rhythmic *PhBmal1*$^{\Delta/\Delta}$ animals, the periods were abnormal, with a wide distribution (Figure 7M), reminiscent of the residual rhythms observed after LD entrainment (Figure 6F and 6L). Examination of the individual traces of rhythmic *PhBmal1*$^{\Delta/\Delta}$ animals revealed that they did not align well with the expected tidal cycles (Figure 7G-L). Periodograms and power measurement showed that these periodicities had reduced statistical significance, and that the residual rhythms were not robust (Figure 7H,J,L,O,P). Our results thus clearly show that the circadian protein PhBMAL1 is critical for the expression of 12.4/24.8 h circatidal rhythms in *P. hawaiensis*.

Discussion

Our work introduces *Parhyale hawaiensis* as a powerful system to study circatidal rhythms using genetic and molecular approaches. Indeed, we demonstrated that their free-running rhythms of swimming meet all three key criteria for circatidal rhythms: they persist in free-running conditions with a period close to 12.4 h, they are entrained by tidal cues and they are temperature-compensated. Moreover, we engineered – to our knowledge – the first circatidal mutant animals by targeting PhBMAL1, a transcription factor also essential for circadian rhythms in a wide range of animals, including, based on our results, *P. hawaiensis*. Our work thus provides direct evidence for a molecular link between circadian and circatidal clocks.

That PhBMAL1 is required for circatidal rhythms might appear surprising at first, since previous work indicated that core circadian clock proteins are not required for circatidal behaviors. In *E. pulchra*, PER downregulation had no impact on circatidal swimming rhythms, while in *A. asahinai* circatidal locomotor activity was unaffected by both PER and CLK downregulation [25-27]. There are several potential explanations for this apparent contradiction. First, we targeted PhBMAL1, and this transcription factor could be interacting with partners other than CLK to bind DNA. In addition, it may be inhibited by repressors other than PER and CRY2. Indeed, mBMAL1 has been shown to dimerize not just with mCLK, but also with Neuronal PAS domain protein 2 (NPAS2) and Hypoxia Inducible Factor (HIF)-family members [61]. Thus, it is possible that circadian and circatidal clocks share some elements such as PhBMAL1 and PhCkIδ/ε, but use some specific components in order to generate either 12.4 h or 24 h oscillations. Additionally, work in *E. pulchra* and *A. asahinai* was based on RNAi mediated by dsRNA injection, which might not have sufficiently reduced PER or CLK expression in the appropriate cell types. In our studies, knocking out a single *Bmal1* allele was insufficient to affect circatidal rhythms. However, consistent with our results, a recent pre-print reports that injection of dsRNAs targeting *E. pulchra Bmal1* causes a reduction in the percentage of rhythmic animals [62]. We strongly favor the idea that PhBMAL1 is an integral component of the *P. hawaiensis* circatidal clock; however, we cannot eliminate the possibility that it is necessary for the entrainment or expression of

circatidal swimming behavior, without being part of the molecular clock itself. It will be informative to disrupt other core circadian clock genes to determine the degree of overlap between the circadian and circatidal clocks.

P. hawaiensis provides unique opportunities to dissect circatidal behaviors and their entrainment. Indeed, we have established a simple approach to entrain *P. hawaiensis'* circatidal swimming rhythms, which means that the physical parameters that drive entrainment can now be explored, and the sensory systems and neural input pathways mapped. Moreover, circatidal reporter transgenes should be reasonably easy to generate by identifying genes expressed with robust circatidal patterns or through further identification of circatidal transcription factors. This should facilitate the study of circatidal rhythms throughout the body of *P. hawaiensis*, and help to identify circatidal pacemaker neurons. However, it should be noted that *P. hawaiensis'* swimming activity displays high frequency bursts of activity outside of circatidal rhythms. While this has been observed with other marine organisms [63,64], such behavioral "noise" can interfere with circatidal rhythm observation, and might explain why about 20 to 30% of animals are arrhythmic after entrainment to artificial tides. In addition, we noticed that some animals on occasion temporarily suppress their activity, which again could increase arrhythmicity. In spite of these modest drawbacks, *P. hawaiensis* has the potential to be to circatidal rhythms what *Drosophila* has been to circadian rhythms [37].

Interestingly, *P. hawaiensis* exhibits distinctly different rhythmic behavior when animals are exposed only to LD cycles. The period is shorter and activity trends towards unimodality, rather than having two peaks of activity per day. The behavioral phase is also different. In other words, locomotor rhythms appeared better adapted to a diurnal environment after LD-only entrainment. However, a significant fraction of animals still showed two peaks of activity per day. This could indicate a common mechanism underlying circadian and circatidal rhythms, one that is modulated as a function of the inputs that are present. Indeed, it is conceivable that in the wild, *P. hawaiensis* living in shallow waters such as those of mangroves [35] are exposed to prolonged period of submersion or absence of water, depending on tidal amplitude, which varies during the lunar month and over the calendar year. A single, flexible clock that can track both tidal and daily environmental cues, and adapt behavior accordingly,

as proposed by Enright [15], could be a simpler evolutionary solution than a dual-oscillator system. However, circadian and circatidal behavioral components have been detected simultaneously in *E. pulchra* and *A. asahinai* [25,65]. Strong evidence for the existence of distinct circadian and circatidal clocks in *P. hawaiensis* is their differential response to constant light. While the period of circatidal rhythms was insensitive to LL, that of circadian rhythms became longer and more variable. Thus, neurons controlling rhythmic swimming behavior either carry two different molecular timers, one sensitive to light and the other one to tides, or are composed of two distinct populations that control the specific rhythms.

Interestingly, although most *PhBmal1* mutant animals are arrhythmic after tidal entrainment or exhibit improper behavioral periodicities, they nevertheless show a well-defined peak of activity during the first circatidal cycle that occurs at the proper time. This observation strengthens our hypothesis that loss of PhBMAL1 function disrupts the circatidal pacemaker. Indeed, since mutant animals can synchronize their behavior to produce one coherent peak of activity under constant conditions, it seems unlikely that input or output pathways are disrupted by the *PhBmal1*$^{\Delta}$ mutation. Presumably, this single peak reflects the existence of an “hourglass” mechanism, in which animals are able to measure the time that separates them from the last high or low tide, and thus coordinate their activity accordingly [66]. The nature of this hourglass mechanism is unclear, but could be promoted by social cues, since mutant, heterozygous and wild-type organisms were housed together. A similar phenomenon occurs in both *mPer1/mPer2* and *mCry1/mCry2* double-mutant mice, wherein the timing of the first activity bout after release into free-running conditions is accurately timed to the previous diurnal regimen [67,68]. The timing of arginine-vasopressin release by the suprachiasmatic nucleus, a molecular output of the mammalian circadian clock, is also maintained through the first day of free-running conditions in *mPer1/mPer2* double-mutant mice [69].

Some mutant animals also remained weakly rhythmic for days, after either LD or tidal entrainment. These residual rhythms showed a similarly wide range of periodicities after either entrainment protocol. It therefore appears that in the absence of functional circatidal and circadian clocks, some animals can adopt weak behavioral rhythms, whose periods are determined by as yet unknown factors. We cannot entirely exclude

the possibility that the truncated PhBMAL1 protein produced by the mutant allele retained very weak activity sufficient to drive weak rhythms. We see that as unlikely, as previous studies in various systems have demonstrate the requirement of the PAS-B and C-terminal domains for *Bmal1* function [25,49-54,70], and we found no evidence that the truncated PhBMAL1 protein retains any residual transcriptional activity when expressed in heterologous cells.

In summary, our work demonstrates the potential for *P. hawaiensis* to become a workhorse for the study of circatidal rhythms. It is pliable to both gene knockout and transgenesis [71] and exhibits robust circatidal rhythms. We also demonstrate that *PhBmal1* is a molecular link between circadian and circatidal clocks. Future work will explore the nature of this link, and the degree of overlap between the circadian and circatidal clocks. We anticipate that novel mechanisms will emerge, perhaps revealing unexpected plasticity and diversity of the molecular mechanisms underlying biological rhythms in the circadian and ultradian range.

Acknowledgement:

We are also grateful to N. Patel and his lab, in particular E. Alberstat, at the MBL in Woods Hole for providing *Parhyale hawaiensis* colonies, and for their help and advice on CRISPR/Cas9 mutagenesis and animal care. We are additionally grateful to H. Melikian and her lab for their help and advice on genomic DNA extraction and cell culture experiments. This work was supported by a MIRA award from the National Institute of General Medicine Sciences (1R35GM118087) to P.E., a Whitman Research Fellowship from the Marine Biological Laboratory to P.E., and NSF grant #1723141 to J.R., as well as NSF grant #2139765 to P.E. and J.R.

Author Contributions:

Conceptualization: E.K., Y.S., P.E., J.R. Methodology: E.K., Y.S., P.E., J.R. Investigation: E.K, Y.S. Writing -Original Draft: E.K. Writing- Review & Editing: E.K, Y.S., P.E., J.R. Funding Acquisition: P.E., J.R. Supervision: P.E., J.R.

Declaration of Interests:

The authors declare no competing interests.

Inclusion and Diversity:

We support inclusive, diverse, and equitable conduct of research

Figure Legends

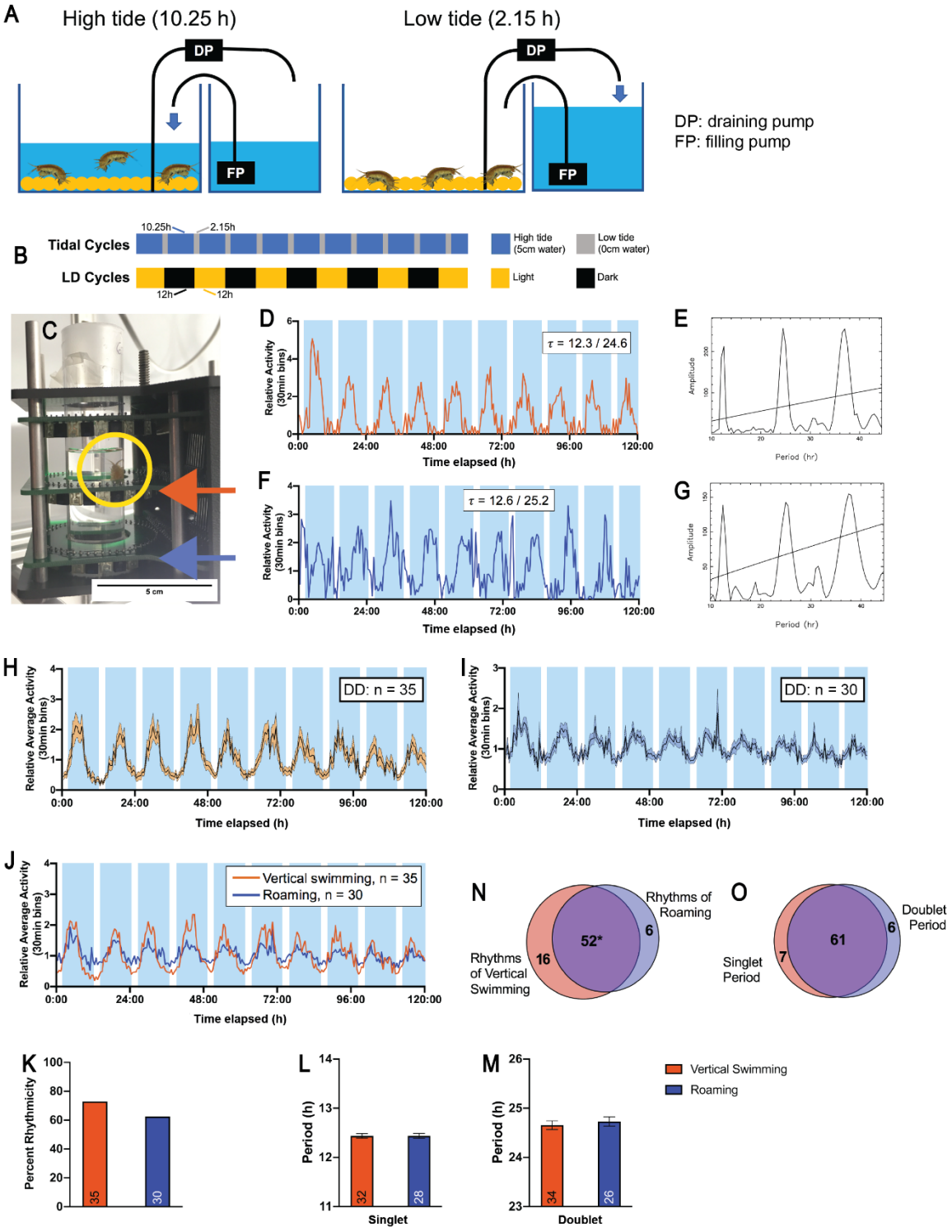
A
High tide (10.25 h)
Low tide (2.15 h)
DP
FP
DP: draining pump
FP: filling pump
B
Tidal Cycles
LD Cycles
10.25h
2.15h
12h
12h
High tide (5cm water)
Low tide (0cm water)
Light
Dark
C
5 cm
D
τ = 12.3 / 24.6
Relative Activity (30min bins)
Time elapsed (h)
E
Amplitude
Period (hr)
F
τ = 12.6 / 25.2
G
H
DD: n = 35
Relative Average Activity (30min bins)
I
DD: n = 30
J
Vertical swimming, n = 35
Roaming, n = 30
N
Rhythms of Roaming
Rhythms of Vertical Swimming
52*
16
6
O
Doublet Period
Singlet Period
61
7
6
K
Percent Rhythmicity
35
30
L
Period (h)
Singlet
32
28
M
Doublet
34
26
Vertical Swimming
Roaming

Figure 1. *Parhyale hawaiensis* exhibits rhythms of vertical swimming and roaming after exposure to artificial tidal and LD cycles. (A) *P. hawaiensis* were kept in a tidal tank (left tank) connected to a reserve tank of ASW (right tank). Timed pumps emptied or filled the tidal tank to or from the reservoir tank. During low tide, the tidal tank had no water; during high tide, the water filled to ~5cm. DP: Draining pump. FP: Filling pump. (B) The artificial tides consisted of a 12.4 h period, with 10 h and 15 min of high tide and 2 h and 9 min of low tide. Entrainment consisted of 10 tidal cycles and approximately 5 daily cycle of 12 h of light followed by 12 h dark (12/12 LD). (C) After entrainment, individual *P. hawaiensis* were moved to a behavior tube filled with artificial sea water and placed in a *Drosophila* Population Monitor (DPM) under constant conditions in an incubator. Yellow circle indicates an animal, orange and blue arrows indicate the middle and bottom rings of infrared detectors, respectively. Vertical swimming rhythms were recorded by the middle (orange) detectors, and roaming by the lower (blue) detectors. (D) A representative activity plot of vertical swimming from a male *P. hawaiensis* after entrainment shows robustly rhythmic activity. Activity is plotted beginning at midnight, approximately 4.5 h after transfer of the animals to the DPMs (0:00). Blue shading indicates subjective high tides, white shading indicates subjective low tides, and will throughout this paper. (E) Periodogram of the activity in (D). (F) A representative activity plot of roaming from an individual animal after entrainment. (G) Periodogram of the activity in (F). (H) Average free-running behavior of animals with rhythms of vertical swimming. Standard error is indicated with orange shading. (I) Average free-running behavior of animals with rhythms of roaming, standard error is indicated with blue shading. (J) Relative average activity of rhythmic recordings from the middle (in orange) and bottom (in blue) sensors are shown overlaid. (K) Percentage of animals exhibiting rhythmic activity separated by level is shown. Number of rhythmic animals is indicated by the number at the base of the bars, and will be throughout this paper. No significant difference between the two proportions was found (Fisher's exact test, p-value = 0.3828). (L) and (M) Average singlet (L) and doublet (M) period values do not differ between rhythms detected by the middle sensor (vertical swimming) and the bottom sensor (roaming) (unpaired t-test, p-values = 0.9791 (L) and 0.5676 (M).) Bars indicate SEM, and will be used to do so unless otherwise indicated. (N) Venn diagram for

animals exhibiting rhythms of vertical swimming (VS) and/or roaming (R) * to indicate that of animals exhibiting VS and R rhythms, 37 have a higher-power VS rhythm, while 15 have a higher power R rhythm. (O) Venn diagram for animals exhibiting only a singlet, doublet, or both rhythms. See also Figure S1 and Table S1.

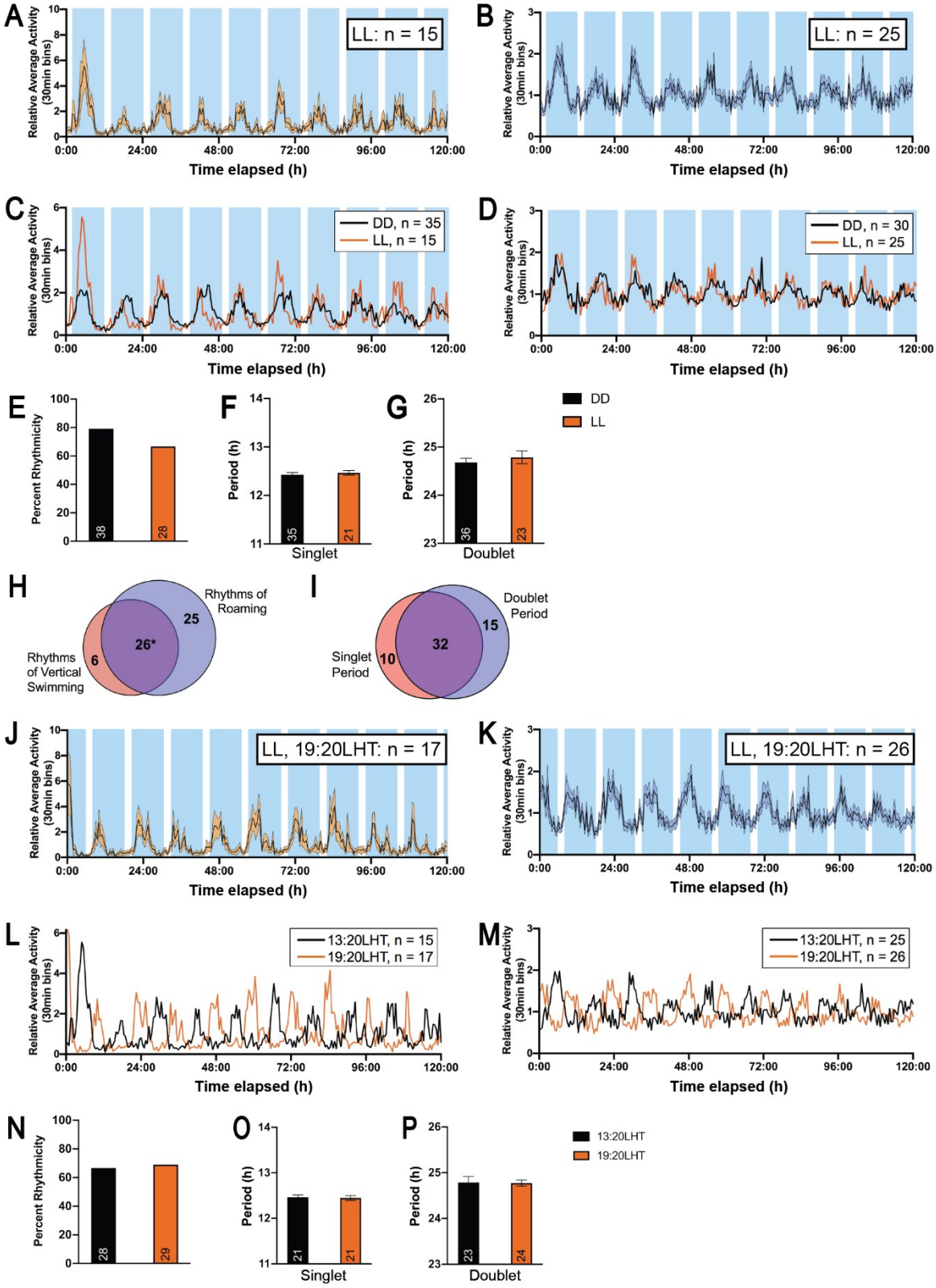
A
LL: n = 15
Relative Average Activity (30min bins)
Time elapsed (h)
B
LL: n = 25
C
DD, n = 35
LL, n = 15
D
DD, n = 30
LL, n = 25
E
Percent Rhythmicity
38
28
F
Period (h)
35
21
Singlet
G
36
23
Doublet
DD
LL
H
Rhythms of Roaming
25
26*
6
Rhythms of Vertical Swimming
I
Doublet Period
15
32
Singlet Period
10
J
LL, 19:20LHT: n = 17
K
LL, 19:20LHT: n = 26
L
13:20LHT, n = 15
19:20LHT, n = 17
M
13:20LHT, n = 25
19:20LHT, n = 26
N
28
29
O
21
21
P
23
24
13:20LHT
19:20LHT

Figure 2. Free-running circatidal rhythms are insensitive to constant light and are entrained by artificial tides. (A,B) Relative average vertical swimming (A) and roaming (B) activity of free-running animals in constant light conditions (LL). SEM and expected tidal cycle represented as in Figure 1. (C,D) Relative average rhythmic vertical swimming (C) and roaming (D) activity in LL (orange) overlaid with the corresponding average activity in DD (black, same traces as in Figure 1). (E) There is no difference in proportion of rhythmic animals between free-running conditions (Fisher's exact test, p-value = 0.2339). (F,G) Average singlet (F) and doublet (G) period values do not differ between rhythms observed in constant dark (black) and constant light (orange) (unpaired t-test, p values = 0.5418 (F) and 0.4594 (G).) (H) Venn diagram for animals exhibiting rhythms of vertical swimming and roaming. * to indicate that of animals exhibiting VS and R rhythms, 12 have a higher power VS rhythm and 14 have a higher power R rhythm. (I) Venn diagram for animals exhibiting only a singlet, doublet, or both rhythms. (J,K) Relative average rhythmic vertical swimming (J) and roaming (K) activity of free-running animals after entrainment to an artificial high tide regimen with the last high tide beginning at 19:20 (LHT 19:20). (L,M) Free-running behavior of animals entrained to a tidal regimen with the last high tide at 13:20 (LHT 13:20) overlaid with that of animals entrained to a tidal regimen with LHT 19:20. (L) shows vertical swimming behavior, and (M) shows roaming behavior. (N) Proportion of rhythmic animals does not differ between differently phased tidal regimens (Fisher's exact test, p-value > 0.999). (O,P) Free-running period values, both singlet (O) and doublet (P), observed after entrainment to differently phased tidal regimens, do not significantly differ (O: Mann-Whitney test, p-value = 0.3399; P: unpaired t-test, p-value = 0.9791 (P).). See also Figure S2, S3 and Table S1.

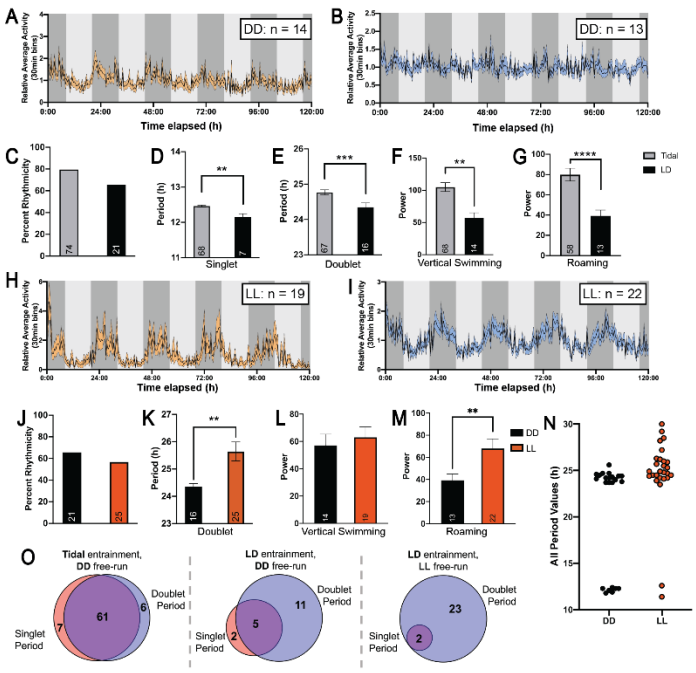

Figure 3. *P. hawaiensis* exhibit circadian rhythms of activity that are distinct from circatidal rhythms. (A,B) Relative average vertical swimming (A) and roaming (B) behavior in free-running conditions (DD) of animals exhibiting rhythmic behavior after entrainment to a LD-only regimen (12:12LD). Behavior is consistent with a primarily crepuscular/nocturnal chronotype, with activity peaking around the expected light-to-dark transition and a broad trough during the expected light period. Plotted behavior includes eight hours of the final dark period before DD began. SEM indicated as in Figure 1. Dark vertical bars indicate subjective night, and light vertical bars indicate subjective day. (C) The proportion of rhythmic animals after LD entrainment trends lower than after tidal entrainment, but there is no significant difference (Fisher's exact test, p-value = 0.1491). (D,E) Average singlet (D) and doublet (E) period values significantly differ between rhythms observed after LD (black) or tidal (grey) entrainment (D: Mann-Whitney test, p-value = 0.0011 (**); E: Mann-Whitney test, p-value = 0.0004 (***).) (F,G) Average power of both vertical swimming (F) and roaming (G) rhythms is significantly reduced after LD entrainment compared to tidal (Mann-Whitney test; p-values = 0.0041 (F,**) and unpaired t-test with Welch's correction: p value < 0.0001 (G,****)). (H,I) Relative average vertical swimming (H) and roaming (I) behavior in constant light (LL) of animals exhibiting rhythmic behavior after LD entrainment. Phase

of behavior is consistent with that observed in DD. Plotted behavior excludes the first four hours of constant light. SEM and subjective day/night indicated as in (A,B). (J) Proportion of rhythmic animals after LD does not significantly differ between LL (orange) and DD (black) conditions (Fisher's exact test, p-value = 0.4834). (K) Average doublet period values are significantly increased in LL compared to DD (Mann-Whitney Test, p = 0.0013, **). Observed variance of doublet periods also significantly differs between LL and DD (not indicated in figure) (F test to compare variances, p < 0.0001). (L,M) Comparison of average power of free-running rhythms of vertical swimming (L) and roaming (M). Roaming power, but not vertical swimming, significantly increases in LL (unpaired t test with Welch's correction; p-values = 0.5970 (L) and 0.0090 (M,**)). (N) All period values resulting from LD entrainment and free-running in DD or LL are plotted. (O) Venn diagram of animals exhibiting only a singlet, doublet, or both rhythms, separated by entrainment to a tidal regimen (left, same diagram from Figure 1O) and entrainment to a LD regimen separated by free-running conditions in DD (middle) and LL (right). See also Figure S4 and Table S1.

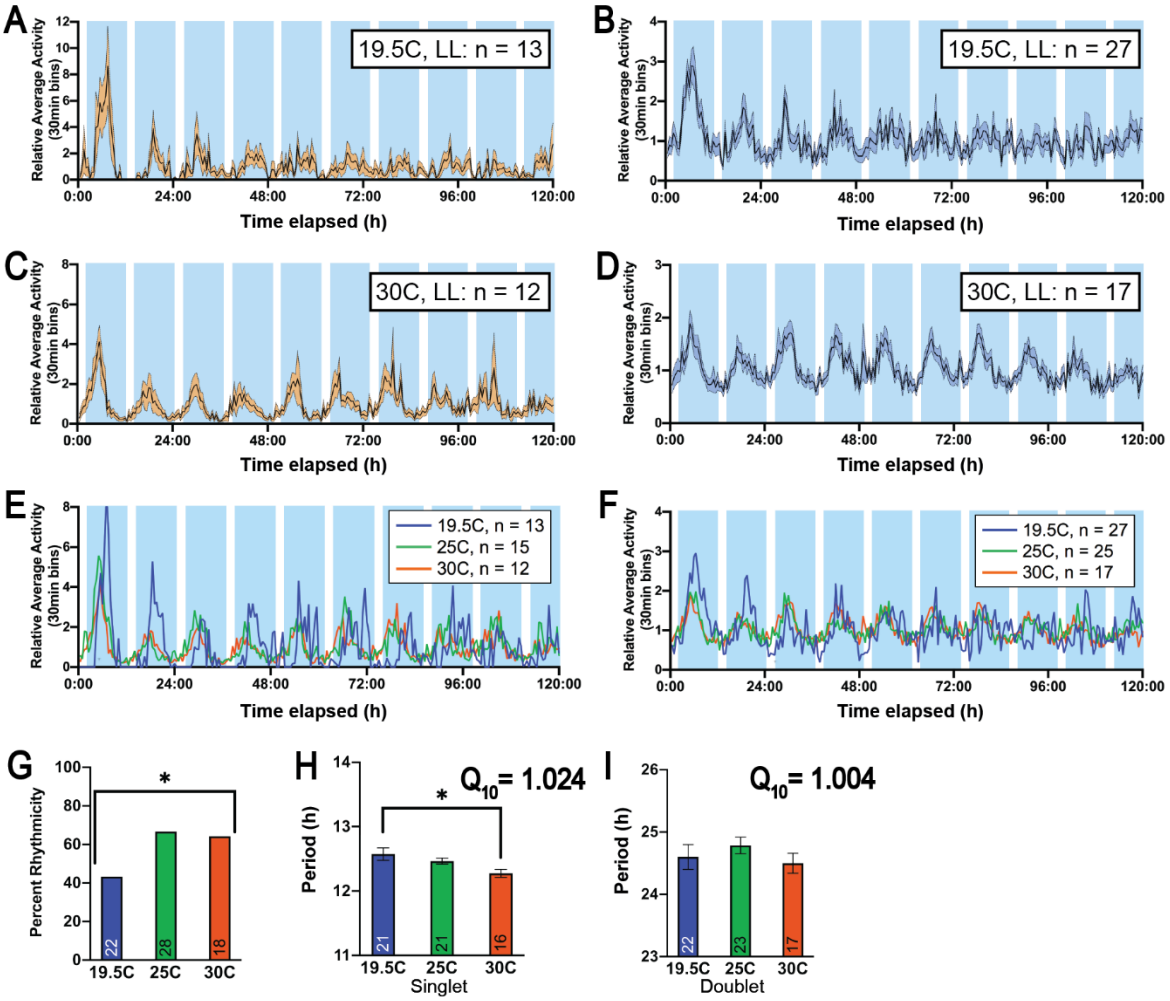

Figure 4. *P. hawaiensis'* circatidal rhythms of swimming are temperature-compensated. (A,B) Relative average vertical swimming (A) and roaming (B) activity of free-running animals at 19.5ºC under LL. SEM and expected tides as represented in figure 1. (C,D) Relative average rhythmic VS (C) and R (D) activity of free-running animals at 30ºC under LL. (E,F) Relative average vertical swimming (E) and roaming (F) activity of free-running animals at 19.5ºC, 25ºC, and 30ºC is overlaid to demonstrate the identical phase of activity peaks and troughs in all three conditions. (G) Free-running rhythmicity decreases significantly with decreasing temperature (Chi-square test, *p-value = 0.0303). (H,I) Average singlet (H) but not doublet (I) period values slightly but significantly differ across the three temperatures (H: Welch's ANOVA, p-value = 0.0179 (not shown), * indicates significance by subsequent multiple comparison, p = 0.0367; G:

Kruskal-Wallis ANOVA, p-value = 0.7225). Calculated Q_{10} values shown. LL-25°C data are the same as those used in figure 2 (LHT13:20). See also Table S1.

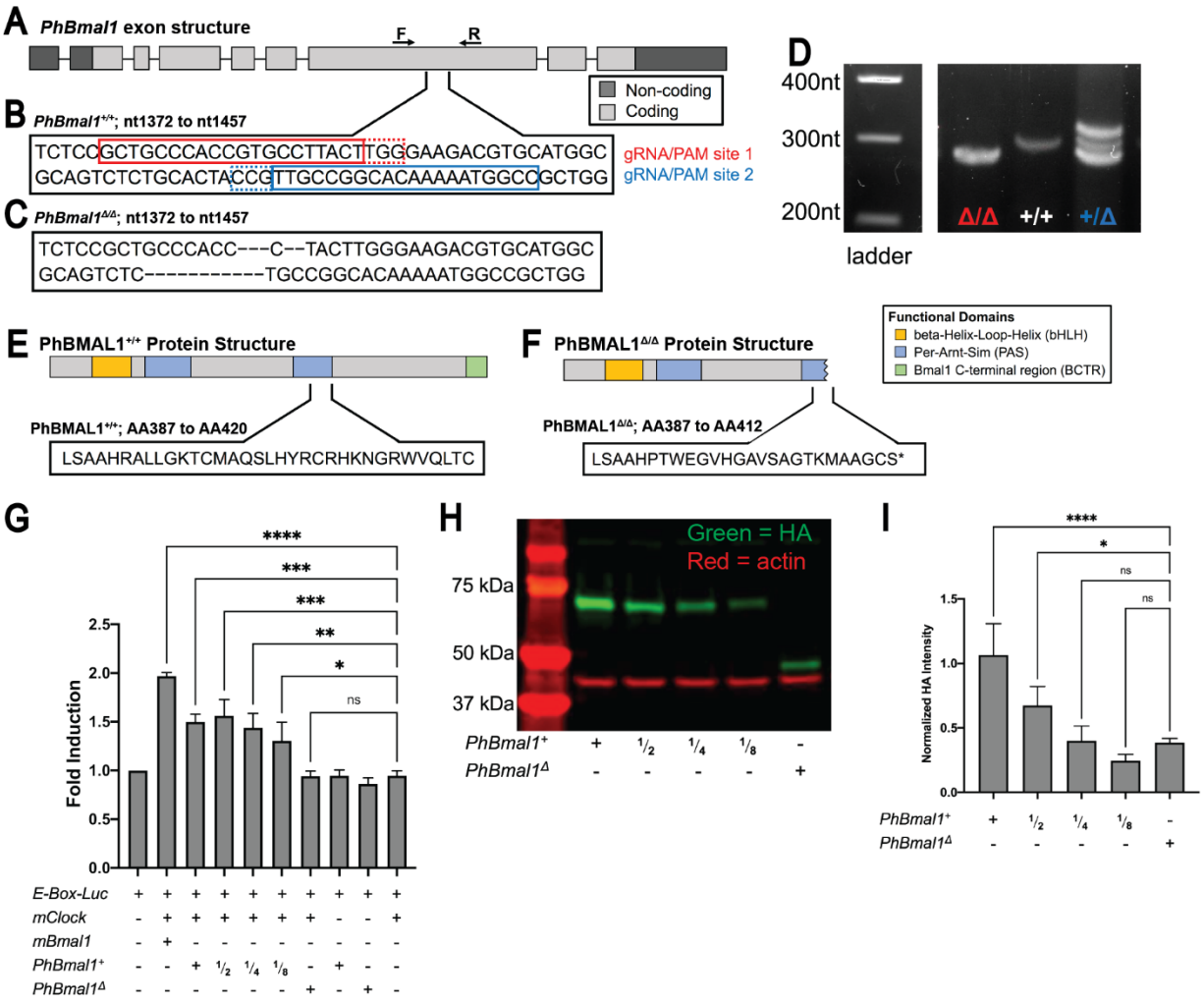

Figure 5. Generation of a loss-of-function allele of *PhBmal1* using CRISPR-Cas9. (A) *PhBmal1* exon structure. The position of the forward (F) and reverse (R) primers used for genotyping are indicated. Exons are drawn to (relative) scale, introns are not. (B) Region of *PhBmal1* targeted by CRISPR-Cas9 mutagenesis, colored boxes indicate sequences used for gRNAs. (C) Sequence of the same region of *PhBmal1* in *PhBmal1*$^{\Delta/\Delta}$ mutant animals. (D) Image of a PCR gel demonstrating the bands generated from (from left to right) *PhBmal1*$^{\Delta/\Delta}$, *PhBmal1*$^{+/+}$, and *PhBmal1*$^{+/\Delta}$ animals.

(E,F) Predicted PhBMAL1 protein structure from the wild-type (E) and *PhBmal1*$^{\Delta}$ (F) alleles. (G) PhBMAL1^{+} and mCLK significantly increase E-box-driven luciferase expression in HEK293 cells, as compared to mCLK alone (Sidak's multiple comparisons test, p = 0.0008 for 0.5 μg [+] of PhBMAL1 plasmid transfected, ***; p = 0.0002 for 0.25 μg [1/2], ***; p = 0.0028 for 0.125 μg [1/4], **; p = 0.0445 for 0.0625 μg [1/8], *). In contrast, PhBMAL1$^{\Delta}$ and mCLK were not able to induce E-box-driven luciferase expression (Sidak's multiple comparisons test, p > 0.9999). As expected, mBMAL1 and mCLK induce E-box-driven luciferase expression significantly (Sidak's multiple comparisons test, p <0.0001, ****). Bars indicate standard error, and represent the average values from 4 independent transfections, each normalized to the negative control (E-box-Luc alone, set to 1). (H) Representative Western Blot probing PhBMAL1^{+} and PhBMAL1$^{\Delta}$ levels in transfected HEK293 cells. Green, HA signal detecting the tagged PhBMAL1 proteins. Red, signal for actin, used as a loading control. (I) Quantification of 4 Western Blots probing PhBMAL1 levels in the protein extracts used for the luciferase assays in (G). When 0.125 μg (1/4) or 0.0625 μg (1/8) of PhBMAL1^{+} is transfected, PhBMAL1^{+} protein abundance does not significantly differ from PhBMAL1$^{\Delta}$ (Dunnett's multiple comparisons test, p-values = 0.9997 (1/4) and 0.4492 (1/8)). When a full (0.5 μg) or half (0.25 μg) amount of PhBmal1^{+} is transfected, there is significantly more PhBMAL1^{+} than PhBMAL1$^{\Delta}$ observed (Dunnett's multiple comparisons test, p-values = <0.0001 (0.5 μg, ****) and 0.0346 (0.25 μg, *)).

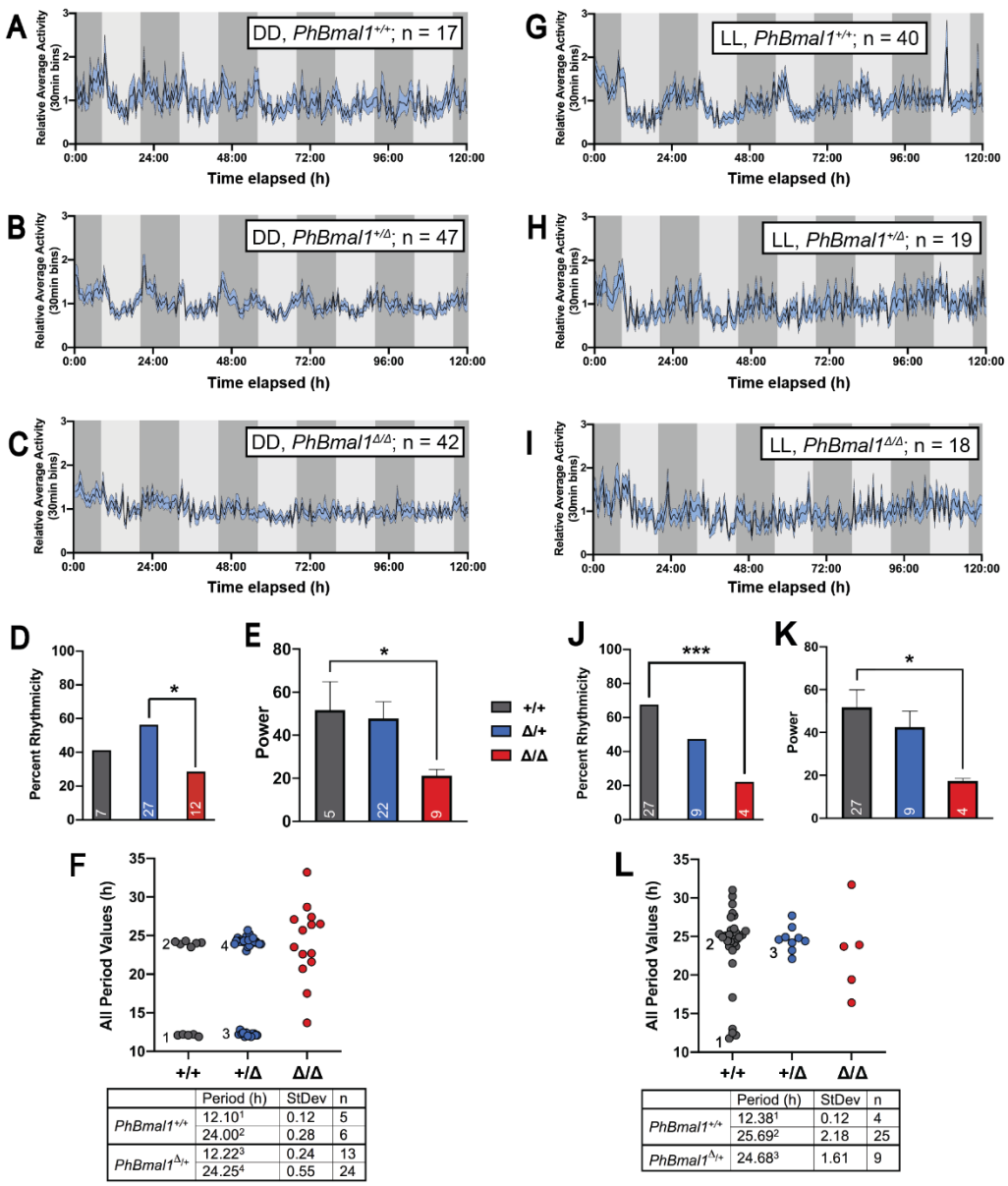

	Period (h)	StDev	n
PhBmal1$^{+/+}$	12.10[1]	0.12	5
	24.00[2]	0.28	6
PhBmal1$^{\Delta/+}$	12.22[3]	0.24	13
	24.25[4]	0.55	24

	Period (h)	StDev	n
PhBmal1$^{+/+}$	12.38[1]	0.12	4
	25.69[2]	2.18	25
PhBmal1$^{\Delta/+}$	24.68[3]	1.61	9

Figure 6. Loss of *PhBmal1* disrupts circadian rhythms. (A,B,C) Relative average roaming activity of all free-running animals in DD; homozygous for the wild-type allele of *PhBmal1* (+/+) (A); heterozygous for the mutant and wild-type alleles (B); and homozygous for the mutant allele (C). SEM and subjective day and night represented as in Figure 1 and 3. (D) Percent rhythmicity does vary significantly by genotype (Chi-square, p = 0.0298 (not shown).) In addition, +/Δ animals were significantly more

rhythmic than Δ/Δ animals (Chi-square with Bonferroni-Holm correction for multiple comparisons, p = 0.0082 (*)). (E) Average power of rhythmic animals does vary significantly by genotype for roaming (Kruskal-Wallis test, p = 0.0227 (not shown), subsequent multiple comparisons showed *PhBmal1*$^{+/+}$ had significantly higher roaming power than *PhBmal1*$^{\Delta/\Delta}$ (Dunn's multiple comparisons, p = 0.0492 (*)). Difference between average roaming power of *PhBmal1*$^{+/\Delta}$ and *PhBmal1*$^{\Delta/\Delta}$ was just over statistical significance (p = 0.0531). (F) All period values resulting from entrainment to a diurnal regimen are plotted for animals with a +/+, +/Δ, or Δ/Δ genotype. Average values for the singlet and doublet period values are shown in the table below for +/+ and +/Δ animals, numbered clusters correspond to superscripts in table. Values did not significantly differ between +/+ and +/Δ animals (singlet: unpaired t-test, p = 0.3001, doublet: unpaired t-test, p = 0.3025). Periods were too widely distributed in homozygous mutant animals for their average to be informative. (G,H,I) Relative average roaming activity of all free-running animals in LL; homozygous for the wild-type allele of *PhBmal1* (G); heterozygous for the mutant and wild-type alleles (H); and homozygous for the mutant allele (I). (J) Percent rhythmicity does vary significantly by genotype (Chi-square, p = 0.0036 (not shown).) In addition, +/+ animals were significantly more rhythmic than Δ/Δ animals (Chi-square with Bonferroni-Holm correction for multiple comparisons, p = 0.0008 (***)). (K) Average power of rhythmic animals does vary significantly by genotype for roaming (Kruskal Wallis test, p = 0.0286 (not shown), subsequent multiple comparisons showed *PhBmal1*$^{+/+}$ had significantly higher roaming power than *PhBmal1*$^{\Delta/\Delta}$ (Dunn's multiple comparisons, p = 0.0243 (*)). (L) All period values resulting from entrainment to a diurnal regimen are plotted for animals with a +/+, +/Δ, or Δ/Δ genotype. Average values for the singlet and doublet period values are shown in the table below for +/+ and +/Δ animals, numbered clusters correspond to superscripts in table. Values did not significantly differ between +/+ and +/Δ animals (unpaired t-test, p = 0.2149 (doublet).) Periods were too widely distributed in homozygous mutant animals for their average to be informative. Note that four homozygous animals were rhythmic out of 18, but one presented two statistically significant periods at 17.4h and 23.7h, hence the five plotted points. See also Figure S5 and S6.

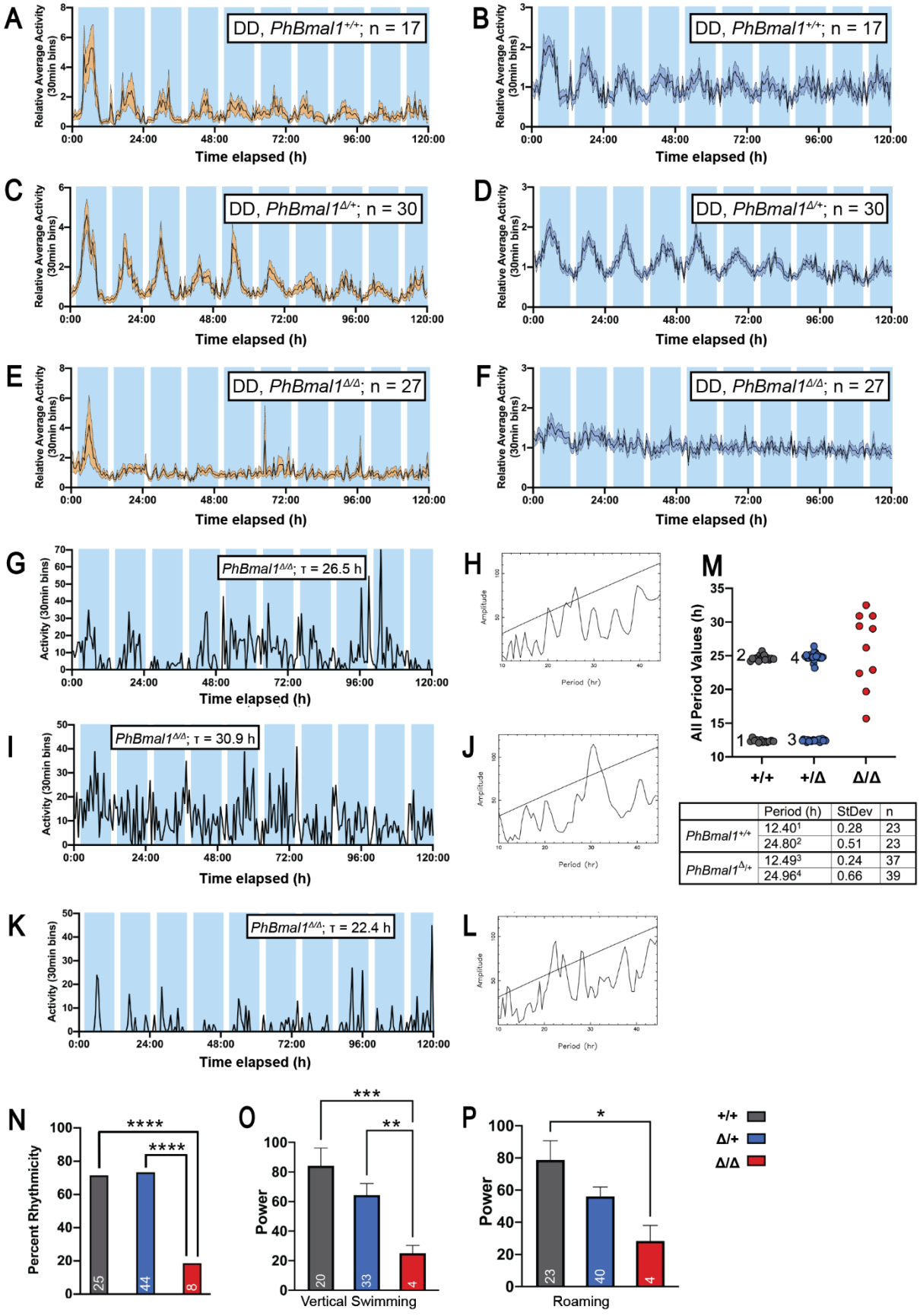

	Period (h)	StDev	n
PhBmal1$^{+/+}$	12.40[1]	0.28	23
	24.80[2]	0.51	23
PhBmal1$^{Δ/+}$	12.49[3]	0.24	37
	24.96[4]	0.66	39

Figure 7. Loss of *PhBmal1* disrupts circatidal rhythms. (A,B) Relative average vertical swimming (A) and roaming (B) activity of all free-running animals homozygous for the wild-type copy of *PhBmal1* (+/+). SEM and expected tidal phase as represented in Figure 1. (C,D) Relative average rhythmic vertical swimming (C) and roaming (D) activity of all free-running animals heterozygous for the mutant and wild-type *PhBmal1* alleles (+/Δ). (E,F) Relative average VS (E) and R (F) activity of all free-running animals homozygous for the mutant *PhBmal1* allele (Δ/Δ). (G,I,K) The free-running vertical swimming activity of three Δ/Δ individuals is shown. (H,J,L) The corresponding periodograms of the Δ/Δ individuals are shown. (M) All period values resulting from entrainment to a tidal regimen are plotted for animals with a +/+, +/Δ , or Δ/Δ genotype. Exact values for the singlet and doublet period values are shown in the table below for +/+ and +/Δ animals. There was no significant difference in values (unpaired t-test, p = 0.1793 (singlet) and 0.3000 (doublet).) Period were too widely distributed in homozygous mutant animals for their average to be informative. (N) Animals lacking a wild-type *PhBmal1* allele display reduced rhythmicity, and proportion of rhythmic animals varies significantly by genotype (Chi-square, p < 0.0001 (not shown)). In addition, Δ/Δ animals were significantly less rhythmic than +/+ and +/Δ animals (Chi-square with Bonferroni-Holm correction for multiple comparisons, p < 0.0001 for both (****)). (O,P) Average power of rhythmic animals significantly varies by genotype for both vertical swimming (O) and roaming (P) activity (Welch's ANOVA, p < 0.0001 (O) and 0.0226 (P) (not shown)). Additionally, both +/+ and +/Δ animals have increased power of vertical swimming rhythms compared to Δ/Δ animals (Dunnett's T3 multiple comparisons; p = 0.0005 (+/+ vs. Δ/Δ, ***) and 0.0013 (+/Δ vs. Δ/Δ, **). Wild-type animals have increased power of roaming compared to Δ/Δ animals (Dunnett's T3 multiple comparisons, p = 0.0156, *).

STAR Methods

Resource Availability

Lead Contact:

Further information and requests for resources and reagents should be directed to and will be fulfilled by the Lead Contact, Patrick Emery [patrick.emery@umassmed.edu].

Materials Availability:

The *P. hawaiensis PhBmal1*$^{\Delta}$ strain and plasmids generated for this manuscript are available upon request to the Lead Contact.

Data and code availability:

- Original data reported in this paper will be shared by the Lead Contact upon request.
- This paper does not report original codes.
- Any additional information required to reanalyze the data reported in this paper will be made available by the lead contact upon request

Experimental Model Details

Animal Husbandry

Wild-type *P. hawaiensis*, of the Chicago F strain, were obtained from N. Patel's lab at the Marine Biological Laboratory and kept in polycarbonate tanks covered almost completely by a blue tinted lid and filled with 5 cm of artificial seawater (Instant Ocean Sea Salt, Instant Ocean, China). The tanks contained approximately 1.5cm of crushed coral substrate, with small pieces of rolled netting to provide enrichment, and the tanks were kept in a temperature-controlled room at 25ºC. Water salinity was maintained at a specific gravity of 1.025, and an air pump (TOM Aquarium Stellar Air Pump W-40, Koller Products, Shawnee, KS) and a submerged airstone provided constant oxygenation. Animals were fed baby carrots once weekly and constantly exposed to a 12:12 h light:dark regimen with ZT0 at 8AM.

CRISPR-Cas9-mediated PhBmal1 Mutagenesis

To collect *P. hawaiensis* embryos for injection, adult females paired with adult males were identified from the population and isolated the day before injections. Mated

females with fertilized embryos were identified from this subset and fertilized embryos were removed by gentle scraping with a curved glass pipet. One or two cell embryos were injected with approximately 40-60 pL of injection mixture as previously described[72]. The injection mixture had a final concentration of 333 ng/μL NLS-Cas9 protein (Synthego Co., Redwood City, CA), 162 ng/μL chemically protected CRISPR gRNAs (one or both guides; Synthego Co., Redwood City, CA), and 0.05% phenol red (Sigma-Aldrich) for visualization during injection. CRISPR gRNAs were designed against regions of the *PhBmal1* gene (shown in Figure 5B) as previously described [33]. (gRNA1 sequence: GGUGCCCACCGUGCCUUACU; gRNA2 sequence: GGCCAUUUUUGUGCCGGCAA). The injected embroys were kept in 6-well plates, placed in an enclosed plastic box with wet paper for humidity. The box was kept in a 27ºC incubator under a 12:12 LD cycle. The embryos were moved with a pipette to new plates with fresh sea water daily. Upon hatching, each individual animal was moved to an isolated well of a 12 well plate and water was changed every other day. After hatching, the animals were given access to 1-2 drops of hatchling food mix for approximately one hour every water change. The hatchling food mix (adapted from Rehm et al.[31] and protocols from the Extavour's lab [https://www.extavourlab.com/wp-content/uploads/2017/10/Parhyale-hawaiensis-culture.pdf]) consisted of approximately 1 tablespoon of ground TetraMin PLUS Tropical Flakes (Tetra, Melle, Germany), ground OSI Spirulina Flake Fish Food (Ocean Star International, Snowville, UT), ground Hikari Wheat Germ Floating Pellets for Pets (Hikari, Japan), and approximately 0.5 tablespoons of ground Nutrafin Max Livebearer and Tubifex (Hagen Group, Quebec, Canada). The dry food mix is kept at room temperature. Before usage, a small amount (enough to cover the surface) of dry food mix was mixed into 30 ml ASW in a 50 ml Falcon tube. This was followed by the addition of 5 ml American Marine Selcon Vitamin Supplement (American Marine Inc., Ridgefield, CT) and 5 ml KENT Marine Zoe Marine Vitamin (KENT Marine, Franklin, WI). The mixture was then shaken and kept at 4ºC for up to one week.

Once injected animals reached sexual maturity, they were paired with wild-type members of the opposite sex and allowed to mate freely. Cultures were kept in glass pyrex bowls with oxygenating air pumps and 1.5cm of substrate, and water was

changed twice weekly. Cultures were transitioned from the hatchling food mix to baby carrots as a food source for their maintenance.

To screen for *PhBmal1* mutants, adult animals were anesthetized using clove oil in ASW at a 1:5000 dilution. Once anesthetized, a pair of appendages was removed from the animals with forceps and placed in 250μL of lysis buffer (100mM Tris, 5mM EDTA, 200mM NaCl, 0.2% SDS, 100μg/μL Proteinase K) and kept overnight on a rotating rack at 50°C. The following day, the solutions were spun down at 13,000RPM for 10 minutes at 4°C. 200μL of supernatant was mixed with an equal volume of isopropanol and inverted several times before being centrifuged again at 13,000RPM for 3 minutes at room temperature. The supernatant was removed and discarded, and the pellet washed with 500μL of 70% ethanol. Following 1 minute of centrifugation at room temperature, the supernatant was again discarded and the remaining pellet was allowed to dry at 50°C until no liquid was left. gDNA was then suspended in 20μL of molecular grade water and the concentration and quality determined using a NanoDrop 2000c apparatus (ThermoScientific). The resulting gDNA was used in a PCR reaction with primers located ~150bp upstream and downstream of the gRNA target sites (forward primer: CAGAAGCCAAGTACAGCT; reverse primer: CGGCAATACGCTATTACTG (Integrated DNA Technologies)). *Taq* DNA polymerase (New England BioLabs) was used to amplify products using an amplification program of 35 cycles of 95°C for 30s, 46°C for 30s, and 68°C for 20s. PCR products were then run on a 2.5% agarose gel, isolated and sequenced. From each of the five colonies that were generated from different injected animals, a minimum of 15 individuals were genotyped to verify presence or absence of mutations. Multiple individuals from a single colony turned out to carry a mutant *PhBmal1* allele (*PhBmal1*$^{\Delta}$).

Method Details

Tidal entrainment and behavioral monitoring under constant conditions

Tidal entrainment consisted of ten artificial tidal cycles of 10.3:2.1 h high tide: low tide. Low tide was generated by draining the animal tank into an adjacent reservoir using a submerged tube covered in fine netting, until there was no pooled water left (the

substrate, however, remained damp). High tide was produced by pumping the water in the reservoir back into the animal tank through a tube placed in the lid. Each pump was controlled by a timer. The drain pump (TOM Aquarium Aqua Lifter 3.5gph, Koller Products, Shawnee, KS,) was activated for 15min and the fill pump (Pulaco 10W 160GPH Submersible Pump, Purelake Group, China) was activated for 1min. For behavioral observations, animals were collected from the tank between 4:30PM and 7:30PM on the last day of entrainment by scooping with a 50ml falcon tube and placed into a polystyrene vial (95mm tall and 25mm in diameter; Genesee Scientific, San Diego, CA) with ~2mm of ground coral substrate and ~5cm of artificial sea water, adjusted to the height of the water and salinity of the entrainment tank ASW (~1.028). A piece of ParaFilm was used to cover the vials to prevent evaporation during free-running.

The tubes with the animals were then loaded into vertically oriented *Drosophila* Population Monitors (DPMs, TriKinetics, Waltham MA) located in a temperature and light-controlled incubator (I36LL, Percival Scientific, Iowa). Swimming behavior was monitored using a TriKinetics Drosophila Activity Monitoring (DAM) system, with activity counts sampled every minute. For constant darkness (DD) conditions, incubator lights were turned off at 20:00, the time at which lights were turned off during entrainment. For constant light (LL), lights were instead kept constantly on after 20:00. Incubator temperature was set at 19.5ºC, 25ºC, or 29ºC.

LD-only entrainment and behavioral monitoring under constant conditions

Animals entrained only to LD cycles (under constant immersion) were placed into vials in an identical fashion to animals entrained to artificial tides. Once loaded into DPMs, animals were subjected to two additional full LD cycles, with the same light-on and -off times. Lights were then turned off permanently to measure rhythms in DD or left on to measure rhythms in constant light (LL).

Behavior analysis

Breaks in the infrared beams of the DPM was used as a surrogate to measure swimming activity. Beam break counts were collected in 30-minute bins and plotted

over time. Analysis of rhythmicity and period length were made using the FaasX software (https://neuropsi.cnrs.fr/en/cnn-home/francois-rouyer/faas-software/, courtesy of F. Rouyer, Centre National de la Recherche Scientifique, Gif-sur-Yvette, France) [73]. Animals were considered rhythmic if they exhibited a period shorter than 34 h, the "power" reached at least 10, and "width" at least 2 (= 1 h), as determined from χ^2 periodogram analysis. Power and width are defined as the height and width (in number of 30 min bins or hours) of a periodogram peak above the statistical significance line. The filter for low frequencies was on.

Periodogram plots were generated with FaasX. Single animal and average activity plots were generated with Graphpad/PRISM. For single or average plots, behavioral activity was normalized within each animal by dividing each 30-min bin value by the bin average activity. These relative average values were then averaged to generate average activity plots for a group of animals.

Entrainment, behavioral monitoring and genotyping of the Bmal1 mutant colony

Once the colony carrying the *PhBmal1*$^{\Delta}$ allele was sufficiently large, it was split into two sub-populations that were entrained either to artificial tides and LD cycles simultaneously, or only to LD, as described above. Animals were then behaviorally monitored, and genotyped by PCR, after behavioral tests as described above.

Luciferase Activity Assay

pcDNA 3.1 plasmids with *mBmal1* and *mClk* cDNA under the control of the CMV promoter were provided by D. Weaver (UMass Chan Medical School) [74]. To produce the *PhBmal1*$^{+}$ and *PhBmal1*$^{\Delta}$ plasmids, the *mClk* plasmid was cut using XhoI and EcoRI. gBlocks (Twist Biosciences) were designed to contain (a) a start codon, (b) an HA tag, (c) either the whole *PhBmal1*$^{+}$ sequence or the *PhBmal1*$^{-}$ allele up to the stop codon introduced by the frameshift mutation flanked by XhoI and EcoRI sites. *Bmal1* fragments were cloned into the cut *mClk* plasmid using these restriction sites. The TK-E54 plasmid [75], which consists of three E-boxes driving expression of firefly luciferase, was also provided by D. Weaver. The c-renilla plasmid was provided by N. Silverman

(UMass Chan Medical School), in which Renilla luciferase expression is driven by the Copia promoter [76].

HEK-293T cells provided by H. Melikian (UMass Chan Medical School) were transfected using Lipofectamine 2000 Transfection Reagent from Invitrogen (Waltham, MA). A total of 2μg of DNA was transfected, with 0.5μg* of *mCLK*, *Bmal1*, TK-E54, and c-renilla plasmids supplemented with empty pcDNA3.1+ when needed (*unless otherwise stated). Cells were plated at 5 x 10^5 cells per well in a 6-well plate, and transfected 24 h after plating. 48 h after transfection, cells were washed using ice-cold PBS (Corning), then lysed using 350μL Passive Lysis Buffer (Promega). Lysed cells were scraped off wells and the lysate was spun down at 13000 rpm. The supernatant was either used immediately for assays or kept at -80 °C.

20μL of each sample were mixed with an equal volume of either D-luciferin (0.132mg/mL D-luciferin (Sigma), 20mM Tricine, 2.67mM $MgSO_4$, 0.1mM EDTA, 33.3mM DTT, 530uM ATP (Sigma), 270uM acetyl coenzyme A (Sigma), 265uM $4MgCO_3$ $Mg(OH)_2$), or coelenterazine (stock at 1mg/mL in ethanol (Biotum, 10110-1)), diluted to 20μg/mL in PBS, on separate black and white 96-well plates (PerkinElmer), and placed in a SpectraMax iD5 microplate reader (Molecular Devices, San Jose, CA) to record luminescence. Firefly luciferase signal was normalized using the renilla luciferase signal. Each data point was the average of four normalized measurements: each transfection mix was used to transfect two wells, and luciferase signals from each well were measured twice.

Western Blotting

Supernatant from cells lysed in Passive Lysis Buffer was treated with 4x Laemmli Sample Buffer (Bio-Rad Laboratories) with 2-mercaptoethanol (Sigma-Aldrich) to a final concentration of 1.05% SDS and 355 mM 2-mercaptoethanol, and boiled at 100°C for 5 minutes. Equal volumes were loaded and proteins resolved on a 4-20% Mini-PROTEAN TGX Stain-Free Protein Gels (Bio-Rad Laboratories). Proteins were transferred to a nitrocellulose membrane using a Trans-Blot® SD Semi-Dry Transfer Cell (Bio-Rad). Membranes were blocked in soy milk for an hour on a shaker at room temperature. Rabbit anti-HA (Cell Signaling Technologies, 1:1000) and mouse anti-actin (Sigma

Aldrich, 1:10000) were used as primary antibodies, and IRDye 680RD Goat anti-rabbit (LI-COR, 1:10,000) and IRDye800 Goat anti-mouse (LI-COR, 1:10,000) were used as secondary antibodies. Imaging was done using an Odyssey DLx Imaging system (LI-COR, Lincoln, NE).

Quantification and Statistical Analysis

GraphPad Prism 9.0 was used to plot graphs and compare independent groups of data. The graphs represent the means ± S.E.M. (unless otherwise mentioned in figure legends). Data were pooled from at least three independent sets of experiments except for circadian behavior in constant dark (two independent sets of experiments), and 'n' represents the biological replicates or total numbers of animals. All the data were tested for normality using the D'Agostino and Pearson omnibus test if the sample size was greater than 20, otherwise, the Shapiro-Wilk test was used. In the case of normally (Gaussian) distributed data, a two-tailed unpaired t-test with or without Welch's correction was used for two groups; for multiple groups, either a one-way ANOVA or Welch's ANOVA (for groups with unequal variances) was used, followed by either a Dunnett's multiple comparisons or Sidak's Multiple Comparison's test for multiple groups. For non-Gaussian distribution, a Mann–Whitney U-test was performed for two groups, while for multiple groups, a Kruskal-Wallis test with Dunn's post-hoc test was performed. For contingency table analyses, Fischer's exact test was used for two groups and Chi-square was used for multiple groups, with subsequent Fischer's exact tests with Bonferroni-Holm correction for multiple comparisons. Statistical significance is demonstrated as ****$P < 0.0001$; ***$P < 0.001$; **$P < 0.01$; *$P < 0.05$.

References

1. Konopka, R.J., and Benzer, S. (1971). Clock mutants of Drosophila melanogaster. Proc Natl Acad Sci U S A *68*, 2112-2116.

2. Zehring, W.A., Wheeler, D.A., Reddy, P., Konopka, R.J., Kyriacou, C.P., Rosbash, M., and Hall, J.C. (1984). P-element transformation with period locus DNA restores rhythmicity to mutant, arrhythmic Drosophila melanogaster. Cell *39*, 369-376.

3. Reddy, P., Zehring, W.A., Wheeler, D.A., Pirrotta, V., Hadfield, C., Hall, J.C., and Rosbash, M. (1984). Molecular analysis of the period locus in Drosophila melanogaster and identification of a transcript involved in biological rhythms. Cell *38*, 701-710.

4. Bargiello, T.A., Jackson, F.R., and Young, M.W. (1984). Restoration of circadian behavioural rhythms by gene transfer in Drosophila. Nature *312*, 752-754.

5. Patke, A., Young, M.W., and Axelrod, S. (2020). Molecular mechanisms and physiological importance of circadian rhythms. Nat Rev Mol Cell Biol *21*, 67-84.

6. Maywood, E.S., O'Neill, J., Wong, G.K., Reddy, A.B., and Hastings, M.H. (2006). Circadian timing in health and disease. Prog Brain Res *153*, 253-269.

7. Nybakken, J.W. (2001). Marine biology : an ecological approach, 5th Edition (Benjamin Cummings).

8. Naylor, E. (2010). Chronobiology of marine organisms (Cambridge University Press).

9. Bohn, G. (1903). Sur les mouvements oscillatoires des Convoluta roscoffensis. Comptes rendus hebdomadaires de l'Acedemie des sciences *173*, 576-578.

10. Gamble, F.W., and Keeble, F. (1903). The bionomics of Convoluta roscoffensis, with special reference to its green cells. Proc. Royal Soc. London *72*, 93-98.

11. Bennett, M.F., Shriner, J., and Brown, R.A. (1957). Peristent tidal cycles of spontaneous motor activity in the fiddler crab, Uca pugnax. Biol. Bull. *112*, 267-275.

12. Rao, K.R. (1954). Tidal rhythmicity of rate of water propulsion in Mytilus and its modification by transplantation. Biol. Bull. *106*, 353-359.

13. Naylor, E. (1997). Crab clocks rewound. Chronobiol Int *14*, 427-430.

14. Palmer, J.D. (1997). Dueling hypotheses: circatidal versus circalunidian battle basics. Chronobiol Int *14*, 337-346.

15. Enright, J.T. (1976). Plasticity in an isopod's clockworks: shaking shapes form and affects phase and frequency. J Comp Physiol *107*, 13-37.

16. Naylor, E. (1958). Tidal and diurnal rhythms of locomotor activityin Carcinus maenas. J Exp Biol *35*, 602-610.

17. Naylor, E. (1996). Crab clockwork: the case for interactive circatidal and circadian oscillators controlling rhythmic locomotor activity of Carcinus maenas. Chronobiol Int *13*, 153-161.

18. Palmer, J.D., and Williams, B.G. (1986). Comparativre studies of tidal rhythms. II. The dual clock control of the lovomotor rhythms of two decapod crustaceans. Mar. Behav. Physiol. *12*, 269-278.

19. Glossop, N.R., Lyons, L.C., and Hardin, P.E. (1999). Interlocked feedback loops within the Drosophila circadian oscillator. Science *286*, 766-768.

20. Shearman, L.P., Sriram, S., Weaver, D.R., Maywood, E.S., Chaves, I., Zheng, B., Kume, K., Lee, C.C., van der Horst, G.T., Hastings, M.H., and Reppert, S.M. (2000). Interacting molecular loops in the mammalian circadian clock. Science *288*, 1013-1019.

21. Emery, P., and Reppert, S.M. (2004). A rhythmic Ror. Neuron *43*, 443-446.

22. Tran, D., Perrigault, M., Ciret, P., and Payton, L. (2020). Bivalve mollusc circadian clock genes can run at tidal frequency. Proc Biol Sci *287*, 20192440.

23. Zurl, M., Poehn, B., Rieger, D., Krishnan, S., Rokvic, D., Veedin Rajan, V.B., Gerrard, E., Schlichting, M., Orel, L., Coric, A., et al. (2022). Two light sensors decode moonlight versus sunlight to adjust a plastic circadian/circalunidian clock to moon phase. Proc Natl Acad Sci U S A *119*, e2115725119.

24. Hafker, N.S., Andreatta, G., Manzotti, A., Falciatore, A., Raible, F., and Tessmar-Raible, K. (2023). Rhythms and Clocks in Marine Organisms. Ann Rev Mar Sci *15*, 509-538.

25. Zhang, L., Hastings, M.H., Green, E.W., Tauber, E., Sladek, M., Webster, S.G., Kyriacou, C.P., and Wilcockson, D.C. (2013). Dissociation of circadian and circatidal timekeeping in the marine crustacean Eurydice pulchra. Curr Biol *23*, 1863-1873.

26. Takekata, H., Matsuura, Y., Goto, S.G., Satoh, A., and Numata, H. (2012). RNAi of the circadian clock gene period disrupts the circadian rhythm but not the circatidal rhythm in the mangrove cricket. Biol Lett *8*, 488-491.

27. Takekata, H., Numata, H., Shiga, S., and Goto, S.G. (2014). Silencing the circadian clock gene Clock using RNAi reveals dissociation of the circatidal clock from the circadian clock in the mangrove cricket. J Insect Physiol *68*, 16-22.

28. Kloss, B., Price, J.L., Saez, L., Blau, J., Rothenfluh, A., Wesley, C.S., and Young, M.W. (1998). The Drosophila clock gene double-time encodes a protein closely related to human casein kinase Iepsilon. Cell *94*, 97-107.

29. Price, J.L., Blau, J., Rothenfluh, A., Abodeely, M., Kloss, B., and Young, M.W. (1998). double-time is a novel Drosophila clock gene that regulates PERIOD protein accumulation. Cell *94*, 83-95.

30. Lowrey, P.L., Shimomura, K., Antoch, M.P., Yamazaki, S., Zemenides, P.D., Ralph, M.R., Menaker, M., and Takahashi, J.S. (2000). Positional syntenic cloning and functional characterization of the mammalian circadian mutation tau. Science *288*, 483-492.

31. Rehm, E.J., Hannibal, R.L., Chaw, R.C., Vargas-Vila, M.A., and Patel, N.H. (2009). The crustacean Parhyale hawaiensis: a new model for arthropod development. Cold Spring Harb Protoc *2009*, pdb emo114.

32. Kao, D., Lai, A.G., Stamataki, E., Rosic, S., Konstantinides, N., Jarvis, E., Di Donfrancesco, A., Pouchkina-Stancheva, N., Semon, M., Grillo, M., et al. (2016). The genome of the crustacean Parhyale hawaiensis, a model for animal development, regeneration, immunity and lignocellulose digestion. Elife *5*. e20062

33. Farboud, B., Jarvis, E., Roth, T.L., Shin, J., Corn, J.E., Marson, A., Meyer, B.J., Patel, N.H., and Hochstrasser, M.L. (2018). Enhanced Genome Editing with Cas9 Ribonucleoprotein in Diverse Cells and Organisms. J Vis Exp. May 25;(135):57350

34. Barnard, J.L., and Karaman, G.G. (1991). The families and genera of marine gammaridean Amphipoda (except marine gammaroids). Rec. Aust. Mus. Suppl. *13*, 1-866.

35. Poovachiranon, S., Boto, K., and Duke, N. (1986). Food preference studies and ingestion rate measurements of the mangrove amphipod Parhyale hawaiensis J Exp Mar Biol Ecol *98*, 129-140.

36. Hunt, B.J., Mallon, E.B., and Rosato, E. (2019). In silico Identification of a Molecular Circadian System With Novel Features in the Crustacean Model Organism Parhyale hawaiensis. Front Physiol *10*, 1325.

37. Hardin, P.E. (2011). Molecular genetic analysis of circadian timekeeping in Drosophila. Adv Genet *74*, 141-173.

38. Griffin, E.A., Jr., Staknis, D., and Weitz, C.J. (1999). Light-independent role of CRY1 and CRY2 in the mammalian circadian clock. Science *286*, 768-771.

39. Kume, K., Zylka, M.J., Sriram, S., Shearman, L.P., Weaver, D.R., Jin, X., Maywood, E.S., Hastings, M.H., and Reppert, S.M. (1999). mCRY1 and mCRY2 are essential components of the negative limb of the circadian clock feedback loop. Cell *98*, 193-205.

40. Darlington, T.K., Wager-Smith, K., Ceriani, M.F., Staknis, D., Gekakis, N., Steeves, T.D., Weitz, C.J., Takahashi, J.S., and Kay, S.A. (1998). Closing the

circadian loop: CLOCK-induced transcription of its own inhibitors per and tim. Science *280*, 1599-1603.

41. Akiyama, T. (2014). Circatidal and circadian rhythms in crustacean swimming behavior. In Annual, Lunar, and Tidal Clocks: patterns and Mechanisms of Nature's Enigmatic Rhythms, H. Numata, and B. Helm, eds. (Springer), pp. 65-80.

42. Hunt, J. (2016). Advancing molecular crustacean chronobiology through the characterisation of the circadian clock in two malacostracan species, Euphausia superba and Parhyale. Ph.D Thesis. (Univeristy of Leicester).

43. Aschoff, J. (1960). Exogenous and endogenous components in circadian rhythms. Cold Spring Harb Symp Quant Biol *25*, 11-28.

44. Konopka, R.J., Pittendrigh, C., and Orr, D. (1989). Reciprocal behaviour associated with altered homeostasis and photosensitivity of Drosophila clock mutants. J Neurogenet *6*, 1-10.

45. Martin-Fairey, C.A., Zhao, P., Wan, L., Roenneberg, T., Fay, J., Ma, X., McCarthy, R., Jungheim, E.S., England, S.K., and Herzog, E.D. (2019). Pregnancy Induces an Earlier Chronotype in Both Mice and Women. J Biol Rhythms *34*, 323-331.

46. Aschoff, J. (1979). Circadian rhythms: influences of internal and external factors on the period measured in constant conditions. Z Tierpsychol *49*, 225-249.

47. Sweeney, B.M., and Hastings, J.W. (1960). Effects of temperature upon diurnal rhythms. Cold Spring Harb Symp Quant Biol *25*, 87-104.

48. de la Iglesia, H.O., and Johnson, C.H. (2013). Biological clocks: riding the tides. Curr Biol *23*, R921-923.

49. Zhang, Y., Markert, M.J., Groves, S.C., Hardin, P.E., and Merlin, C. (2017). Vertebrate-like CRYPTOCHROME 2 from monarch regulates circadian transcription via independent repression of CLOCK and BMAL1 activity. Proc Natl Acad Sci U S A *114*, E7516-E7525.

50. Park, N., Kim, H.D., Cheon, S., Row, H., Lee, J., Han, D.H., Cho, S., and Kim, K. (2015). A Novel Bmal1 Mutant Mouse Reveals Essential Roles of the C-Terminal Domain on Circadian Rhythms. PLoS One *10*, e0138661.

51. Biscontin, A., Wallach, T., Sales, G., Grudziecki, A., Janke, L., Sartori, E., Bertolucci, C., Mazzotta, G., De Pitta, C., Meyer, B., et al. (2017). Functional characterization of the circadian clock in the Antarctic krill, Euphausia superba. Sci Rep *7*, 17742.

52. Kiyohara, Y.B., Tagao, S., Tamanini, F., Morita, A., Sugisawa, Y., Yasuda, M., Yamanaka, I., Ueda, H.R., van der Horst, G.T., Kondo, T., and Yagita, K. (2006). The BMAL1 C terminus regulates the circadian transcription feedback loop. Proc Natl Acad Sci U S A *103*, 10074-10079.

53. Sato, T.K., Yamada, R.G., Ukai, H., Baggs, J.E., Miraglia, L.J., Kobayashi, T.J., Welsh, D.K., Kay, S.A., Ueda, H.R., and Hogenesch, J.B. (2006). Feedback repression is required for mammalian circadian clock function. Nat Genet *38*, 312-319.

54. Chang, D.C., McWatters, H.G., Williams, J.A., Gotter, A.L., Levine, J.D., and Reppert, S.M. (2003). Constructing a feedback loop with circadian clock molecules from the silkmoth, Antheraea pernyi. J Biol Chem *278*, 38149-38158.

55. Xu, H., Gustafson, C.L., Sammons, P.J., Khan, S.K., Parsley, N.C., Ramanathan, C., Lee, H.W., Liu, A.C., and Partch, C.L. (2015). Cryptochrome 1 regulates the circadian clock through dynamic interactions with the BMAL1 C terminus. Nat Struct Mol Biol *22*, 476-484.

56. Fribourgh, J.L., Srivastava, A., Sandate, C.R., Michael, A.K., Hsu, P.L., Rakers, C., Nguyen, L.T., Torgrimson, M.R., Parico, G.C.G., Tripathi, S., et al. (2020). Dynamics at the serine loop underlie differential affinity of cryptochromes for CLOCK:BMAL1 to control circadian timing. Elife *9* e55275.

57. Delwart, E.L., Shpaer, E.G., and Mullins, J.I. (1995). 12 - Heteroduplex Mobility Assays for Phylogenetic Analysis. In PCR Strategies, M.A. Innis, D.H. Gelfand, and J.J. Sninsky, eds. (Academic Press), pp. 154-160.

58. Sgourou, A., Papachatzopoulou, A., Katsila, T., and Patrinos, G.P. (2017). Low- and Medium-Throughput Variant Detection Methods: A Historical Perspective. In Molecular Diagnostics, G.P. Patrinos, ed. (Academic Press), pp. 23-39.

59. Pittendrigh, C.S., Kyner, W.T., and Takamura, T. (1991). The amplitude of circadian oscillations: temperature dependence, latitudinal clines, and the photoperiodic time measurement. J Biol Rhythms *6*, 299-313.

60. Vitaterna, M.H., Ko, C.H., Chang, A.M., Buhr, E.D., Fruechte, E.M., Schook, A., Antoch, M.P., Turek, F.W., and Takahashi, J.S. (2006). The mouse Clock mutation reduces circadian pacemaker amplitude and enhances efficacy of resetting stimuli and phase-response curve amplitude. Proc Natl Acad Sci U S A *103*, 9327-9332.

61. Hogenesch, J.B., Gu, Y.Z., Jain, S., and Bradfield, C.A. (1998). The basic-helix-loop-helix-PAS orphan MOP3 forms transcriptionally active complexes with circadian and hypoxia factors. Proc Natl Acad Sci U S A *95*, 5474-5479.

62. Zhang, L., W., G.E., Webster, S.O., Hastings, M.H., Wilcockson, D., and Kyriacou, C.P. (2023). The circadian clock gene bmal1 is necessary for co-ordinated circatidal rhythms in the marine isopod Eurydice pulchra (Leach). Biorxiv.

63. Neumann, D. (2014). Timing in Tidal, Semilunar, and and Lunar Rhythms. In Annual, Lunar, and Tidal Clocks. , H. Numata, and B. Helm, eds. (Springer), pp. 3-24.

64. Schnytzer, Y., Simon-Blecher, N., Li, J., Waldman Ben-Asher, H., Salmon-Divon, M., Achituv, Y., Hughes, M.E., and Levy, O. (2018). Tidal and diel orchestration of behaviour and gene expression in an intertidal mollusc. Sci Rep *8*, 4917.

65. Satoh, A., Yoshioka, E., and Numata, H. (2008). Circatidal activity rhythm in the mangrove cricket Apteronemobius asahinai. Biol Lett *4*, 233-236.

66. Rensing, L., Meyer-Grahle, U., and Ruoff, P. (2001). Biological timing and the clock metaphor: oscillatory and hourglass mechanisms. Chronobiol Int *18*, 329-369.

67. Zheng, B., Albrecht, U., Kaasik, K., Sage, M., Lu, W., Vaishnav, S., Li, Q., Sun, Z.S., Eichele, G., Bradley, A., and Lee, C.C. (2001). Nonredundant roles of the mPer1 and mPer2 genes in the mammalian circadian clock. Cell *105*, 683-694.

68. Vitaterna, M.H., Selby, C.P., Todo, T., Niwa, H., Thompson, C., Fruechte, E.M., Hitomi, K., Thresher, R.J., Ishikawa, T., Miyazaki, J., et al. (1999). Differential

regulation of mammalian period genes and circadian rhythmicity by cryptochromes 1 and 2. Proc Natl Acad Sci U S A *96*, 12114-12119.

69. van der Veen, D.R., Mulder, E.G., Oster, H., Gerkema, M.P., and Hut, R.A. (2008). SCN-AVP release of mPer1/mPer2 double-mutant mice in vitro. J Circadian Rhythms *6*, 5.

70. Huang, N., Chelliah, Y., Shan, Y., Taylor, C.A., Yoo, S.H., Partch, C., Green, C.B., Zhang, H., and Takahashi, J.S. (2012). Crystal structure of the heterodimeric CLOCK:BMAL1 transcriptional activator complex. Science *337*, 189-194.

71. Kontarakis, Z., and Pavlopoulos, A. (2014). Transgenesis in non-model organisms: the case of Parhyale. Methods Mol Biol *1196*, 145-181.

72. Martin, A., Serano, J.M., Jarvis, E., Bruce, H.S., Wang, J., Ray, S., Barker, C.A., O'Connell, L.C., and Patel, N.H. (2016). CRISPR/Cas9 Mutagenesis Reveals Versatile Roles of Hox Genes in Crustacean Limb Specification and Evolution. Curr Biol *26*, 14-26.

73. Grima, B., Lamouroux, A., Chelot, E., Papin, C., Limbourg-Bouchon, B., and Rouyer, F. (2002). The F-box protein slimb controls the levels of clock proteins period and timeless. Nature *420*, 178-182.

74. Etchegaray, J.P., Lee, C., Wade, P.A., and Reppert, S.M. (2003). Rhythmic histone acetylation underlies transcription in the mammalian circadian clock. Nature *421*, 177-182.

75. Honma, S., Kawamoto, T., Takagi, Y., Fujimoto, K., Sato, F., Noshiro, M., Kato, Y., and Honma, K. (2002). Dec1 and Dec2 are regulators of the mammalian molecular clock. Nature *419*, 841-844.

76. Lum, L., Yao, S., Mozer, B., Rovescalli, A., Von Kessler, D., Nirenberg, M., and Beachy, P.A. (2003). Identification of Hedgehog pathway components by RNAi in Drosophila cultured cells. Science *299*, 2039-2045.

77. Schneider CA, Rasband WS, Eliceiri KW. (2012) NIH Image to ImageJ: 25 years of image analysis. Nat Methods *9*, 671-675.

Key resources table

REAGENT or RESOURCE	SOURCE	IDENTIFIER
Antibodies		
Rabbit monoclonal anti-HA	Cell Signaling Technology	Cat#3724; RRID:AB_1549585
Mouse anti-actin	Sigma Aldrich	Cat#sc-56459; RRID:AB_830981
IRDye 680RD Goat anti-rabbit	LI-COR	P/N 926-68070; RRID AB_10956588
IRDye 800 Goat anti-mouse	LI-COR	P/N 926-32211; RRID AB_621843
Chemicals, peptides, and recombinant proteins		
Sea Salt	Instant Ocean Sea Salt	n/a
NLS-Cas9 protein	Synthego Co.	
Phenol Red	Sigma-Aldrich	n/a
Clove oil (*Syzgium aromaticum*)	Plant Therapy Essential Oil Co.	n/a
Proteinase K	New England BioLabs	Cat# P8107S
Taq DNA Polymerase	New England BioLabs	Cat#M0267S
Lipofectamine 2000 Transfection Reagent	Invitrogen	Cat#11668019
Passive Lysis Buffer	Promega	Cat#PAE1941
D-luciferin	Sigma	Cat#L9504; CAS 2591-17-5
Coelenterazine	Biotium	Cat#10110-1; CAS 55779-48-1
Experimental models: Cell lines		
Human: HEK293T	Haley Melikian, UMass Chan Medical School	
Experimental models: Organisms/strains		
Parhyale hawaiensis, Chicago-F strain	Nipam Patel	
Parhyale hawaiensis, *Bmal1Δ*	This paper	n/a
Oligonucleotides		
PhBmal1 guide RNA #1 (chemically protected): GGUGCCCACCGUGCCUUACU	Synthego Co.	n/a
PhBmal1 guide RNA #2 (chemically protected): GGCCAUUUUUGUGCCGGCAA	Synthego Co.	n/a
PhBmal1 Forward Primer: CAGAAGCCAAGTACAGCT	Integrated DNA Technologies	n/a

PhBmal1 Reverse Primer: CGGCAATACGCTATTACTG	Integrated DNA Technologies	n/a
HA.PhBmal1+ gBlock A: GAATTCATGTACCCATACGATGTTCCAGATTACGCTGCGGC CGCTATGTACAGCACAGGGGGATACAGCAACACACATGCA GAGTATATCTCTGAATGTGGCTCTATCGCTTCCGTCGCCTC CCTGTCTTCTGATGGCATTGCCATGAAAAAGAAAATTCCTG GACATGGAGAGTGCCACAATGAAGATGATTTGGAGTGTAG CAAGCTCGCAAGAAGTTCTGCTGAGTGGAATAAAAGGCAG AACCACAGTGAAATCGAGAAGAGAAGGCGTGATAAAATGAA CACATACATATCGGAGCTGTCACGGATGATCCCACAGTGTC GCAGCCGTAAGCTGGACAAGCTGAGCGTGCTGCGCATGG CTGTGCAGCACATCAAGATGTTGCGAGGTTCGCTTAATTCT TACACTGAAGGCCAGTACAAGCCCGGCTTTGTGACTGATG ATGAGGTGCAGCAGTTGCTCAAACAGGAGTGCTGCGAAAG CTTCTTGTTTGTTGTTGGCTGTGACAGAGGCAAGATC	Twist Biosciences	n/a
HA.PhBmal1+ gBlock B: TTTGTGACTGATGATGAGGTGCAGCAGTTGCTCAAACAGGA GTGCTGCGAAAGCTTCTTGTTTGTTGTTGGCTGTGACAGAG GCAAGATCCTGTTTGTGTCCGAGTCTGTGGCGCACATCCT GCAATACACTCAGCAAGAACTGCTTGGCTCCAGCTGGTTTG ACATTCTGCATCCCAAAGACTTGAACAAAGTTAAGGAACAG TTGTCGTGTGGAGATATGAATCGCAGAGAGCGGCTCGTTG ATGCTAAGACTCTACTGCCAGTACACCAGTCGCCCAACAGC AGCAGTAGCAGCGGCAGCAGTGGCAACTACCCCACCCTGC CCGCCGACCTGACCCGCCTGTGCCCCGGCTCCCGCCGCG CCTTCTATGCACGCATACGCTGCCCCAGTGTCAACAAGGT GCAGTCTGATGACGGTGGTGGTGGAGGTGACAGTGGGAG CGTGTGCGACGAGAGCGTGACCGGGGACAAGCGCTACCT CAGCATACACTTCACTGGGTACCTCAAGAGCTGGCAGGGG GGCCGGCGCGCCTCGTGTGGCGGAGGGGACGATGATCAC GATTTTGGAGATGCTGCTTGTCTGGTAGCCATCGGACGTCT TCACAGACCTCACGCTGACTTCCCTCCGCTGCATTTCATCG CCAAACTCTCGGCAGAAGCCAAGTACAGCTATGTTGATCAG AGAGTGAGTGTAGTGCTGGGCTGGCTGCCACAGGAGATCT TAGGCGCGAGTGTGTTCGAACTGAGCCACCCCAGTGACCA CTCGACTCTCTCCGCTGCCCACCGTGCCTTACTTGGGAAG ACGTGCATGGCGCAGTCTCTGCACTACCGTTGCCGGCACA AAAATGGCCGCTGGGTGCAACTGACCTGTAAGTGGACGCT CTTCACTAACCCATGGACCAATGAGCTGGAGTACATCGTCG CCAGTAATAGCGTATTGCCGTCCTCTCCTGCTCCCGATGAC GCGCTGGGAGATGCCTCCTGTCGCAGTACAGAGCCCGTGA TATCGTCCCCTACTGTGGCCGGCGTCTCGCTGGGTGGTGG GACTTTGGATGTCCGCCCTGCTTCGGTCACCAGCTGCTCC TATGGCGGCGATGCCAAGGCCTTCACTGCTGGGAAGGACA ACCTTAGCTCTGACGCACTTCGAACGCCCCATGACGGGAA GGGGAGCGGCCCTACGGCACGTGATGCCGCCGACTGCCG CACTGGAGCGCACCCACAGCTGTCGGCTGACACTGGCGA GACTGGGGACAACAGTGCACTGCCCCAGCAACTGGACGTC CCCACTCGCCTGCCCTTCCATCATCACTACAACACTCGCAG CGAGTCGGAAGCAAGTGGCGTTGGCGAGACCACCAGCGA CTCCGACGAGGCTGCCATGGCAATTATTATGAGTCTCCTGG AAGCAGATGCTGGCCTGGGCGGTCCTGTGGACTTCAGCCA TCTGCCTTGGCCTCTGCCCTGACTCGAG	Twist Biosciences	n/a
Recombinant DNA		

Plasmid: mouse *Bmal1* (*mBmal1*)	Etchegaray et al.[74]	n/a
Plasmid: mouse *Clock* (*mClk*)	Etchegaray et al.[74]	n/a
Plasmid: *HA-PhBmal1+*	This paper	n/a
Plasmid: *HA-PhBmal1Δ*	This paper	n/a
Plasmid: *TK-E54*	Honma et al.[75]	n/a
Plasmid: *c-renilla*	Lum et al.[76]	n/a
Plasmid: *pcDNA3.1+*	Thermo-Fisher	Cat#V79020
Software and algorithms		
Drosophila Activity Monitoring System	TriKinetics	n/a
FaasX	F. Rouyer, Centre National de la Recherche Scientifique	https://neuropsi.cnrs.fr/en/cnn-home/francois-rouyer/faas-software/
GraphPad/PRISM	GraphPad	n/a
SpectraMax iD5 Microplate Reader	Molecular Devices	n/a
Odyssey DLx Imaging System	LI-COR	n/a
ImageJ	Schneider et al.[77]	https://imagej.nih.gov/ij/
Other		
TOM Aquarium Aqua Lifter Pump (for tidal entrainment setup)	Koller Products	https://www.fishpond.co.il/Pets/TOM-Aquarium-Aqua-Lifter-Pump-35gph-flow-rate-to-80cm-height/0802202662532
Pulaco 10W 160GPH Submersible Pump (for tidal entrainment setup)	Pulaco	https://www.amazon.com/PULACO-Submersible-Aquariums-Hydroponics-Fountains/dp/B07YLHVZ4Q

Supplemental Files

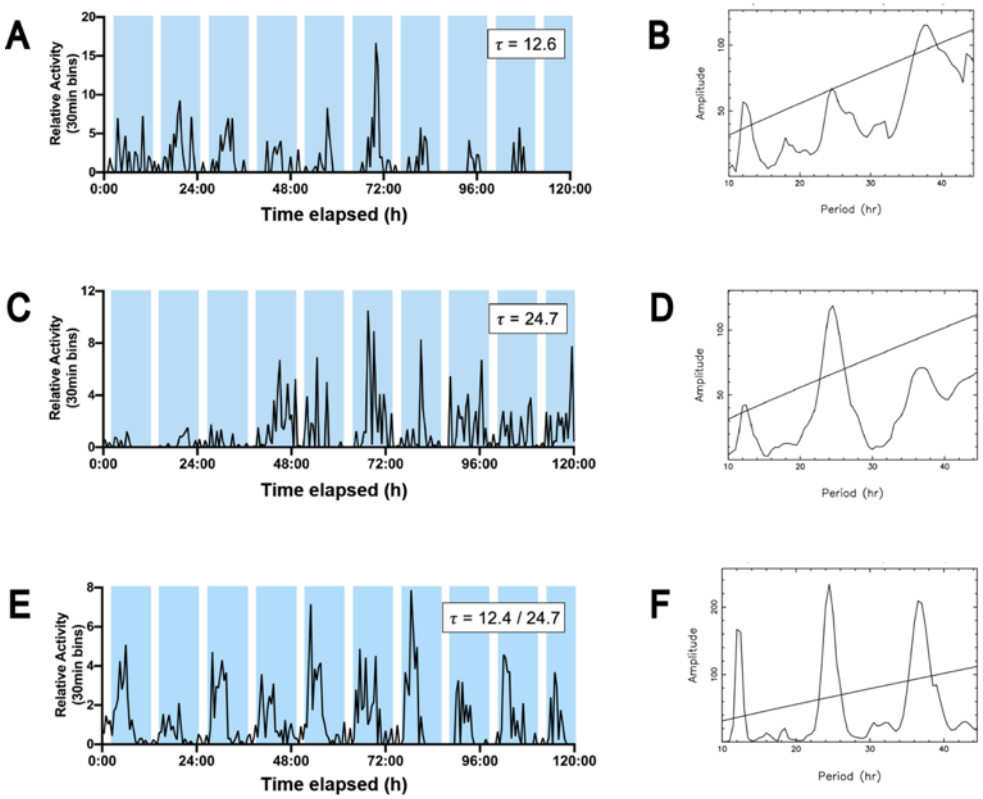

Figure S1. Some *Parhyale hawaiensis* exhibit episodes of inactivity during free-running conditions, related to Figure 1. (A,C,E) Relative activity of a single animal is plotted over the 120 hours following loading. Blue vertical bars indicate expected high tide, white bars indicate expected low tide. Activity plotted in A and C do not exhibit activity peaks for every expected high tide, as compared to activity plotted in E. (B,D,F) The corresponding periodograms indicate that although there are weak peaks where a doublet (B) or singlet (D) should be, they do not reach significance.

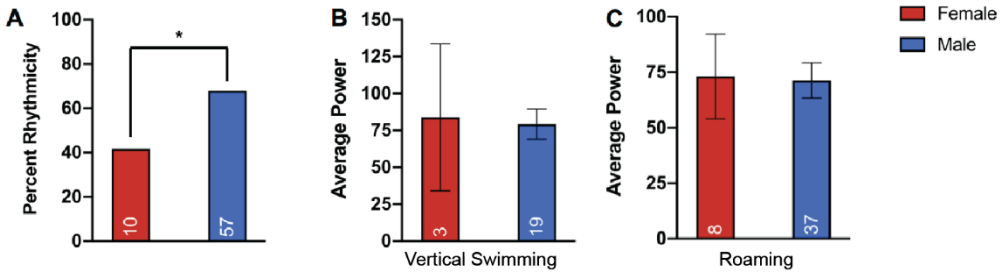

Figure S2. Male *Parhyale hawaiensis* are more likely to exhibit rhythms after circatidal entrainment, related to Figure 2. (A) The proportion of rhythmic females in free-running conditions after entrainment was significantly lower compared to rhythmic males (Fisher's exact test, p = 0.0307). All animals were entrained to a tidal regimen ending at either 13:20 or 19:20, and free-ran in constant light conditions. Number of rhythmic animals is indicated at the base of each column. (B,C) The average power of rhythmic females was not significantly different from males for either vertical swimming or roaming (B: Welch's t-test, p = 0.9356; C: Mann-Whitney Test, p = 0.8728).

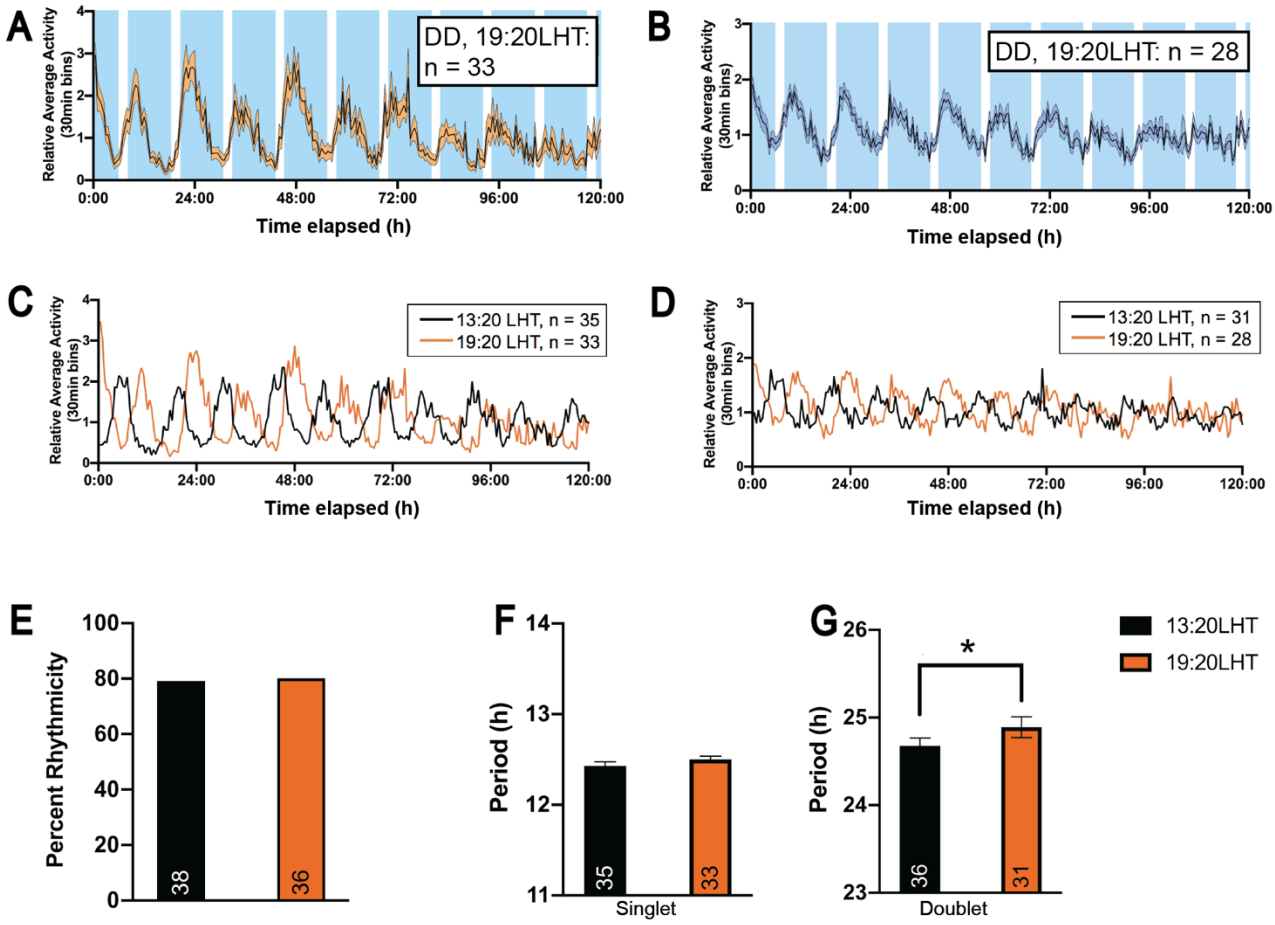

Figure S3. Free-running circatidal rhythms observed in constant dark are entrained by artificial tides, related to Figure 2. (A,B) Relative average vertical swimming (A) and roaming (B) activity of free-running animals in constant dark conditions (DD) after entrainment to an artificial tidal regimen with the last high tide at 19:20 the night before loading (19:20LHT). SEM and expected tidal cycle represented as in Figure 1. (C,D) Relative average rhythmic vertical swimming (C) and roaming (D) activity in DD after entrainment to a tidal regimen with the last high tide at 13:20 (black, LHT 13:20) overlaid with animal entrained to a tidal regimen with LHT 19:20 (orange, same traces as in figure 1). (E) There is no difference in proportion of rhythmic animals between entrainment regimens (Fisher's exact test, p-value >0.9999). (F,G) Average singlet (F) period values did not significantly differ between rhythms observed after 13:20LHT (black) and 19:20LHT (orange), while doublet values (G) barely cleared significance threshold (F: unpaired t-test, p-value = 0.1949; G: Mann-Whitney test, p = 0.0441).

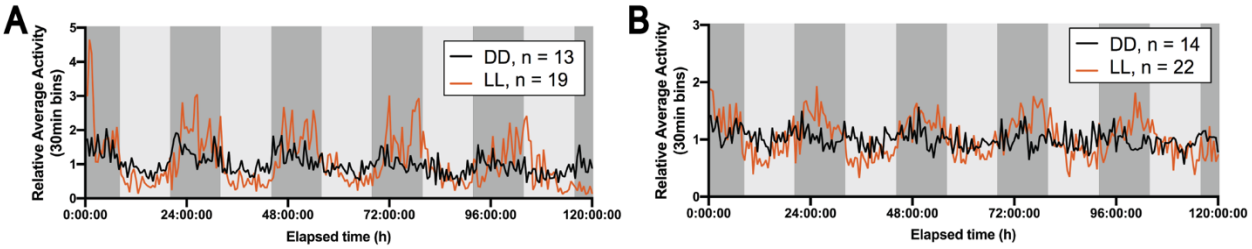

Figure S4. Constant light exposure after LD entrainment lengthens period and increases swimming rhythm amplitude, related to Figure 3. Comparison of average activity under LL and DD for vertical swimming (left) and roaming (right) illustrates the increase in rhythm amplitude under LL.

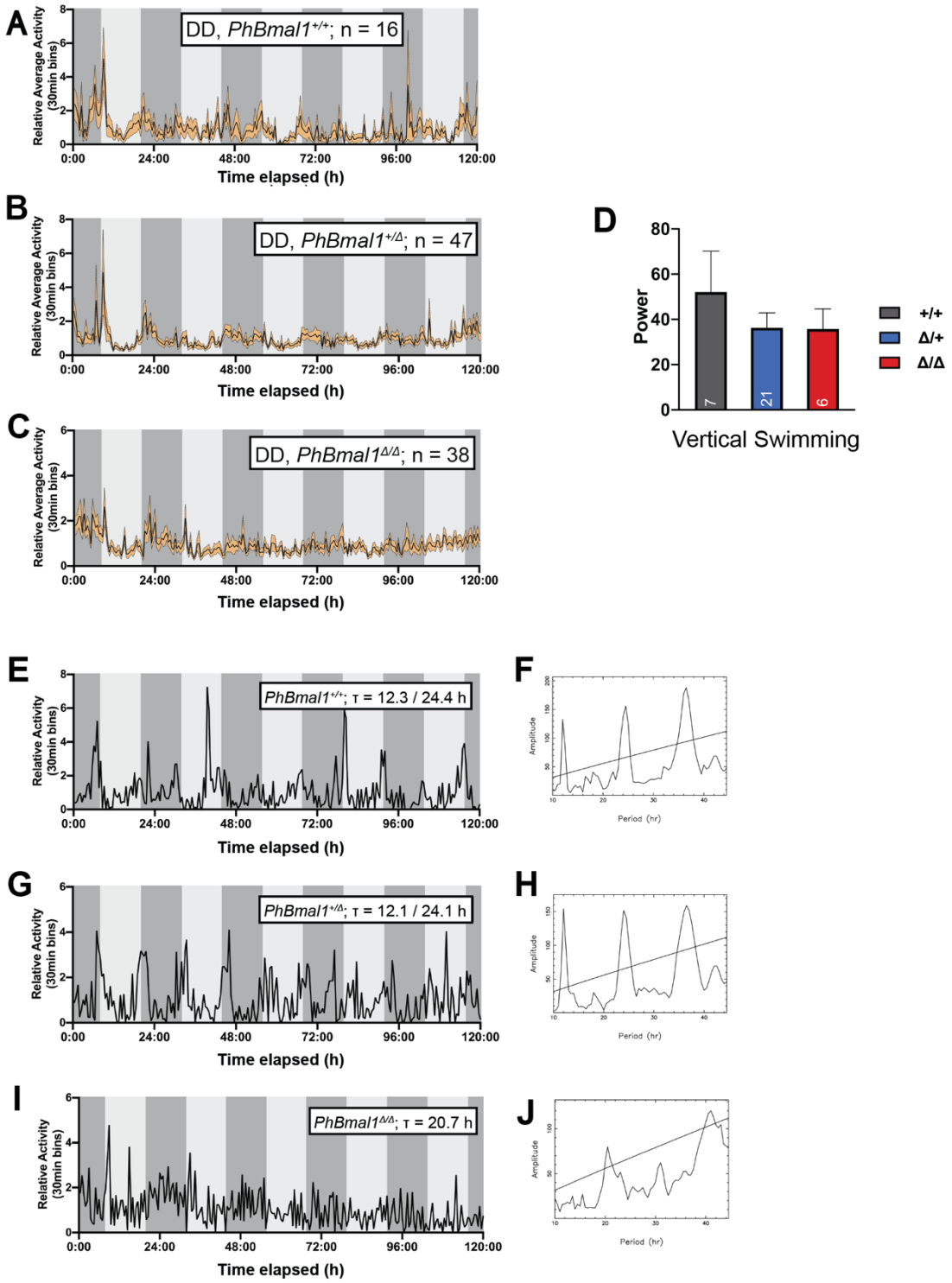

Figure S5. Loss of *PhBmal1* disrupts circadian rhythms in DD, related to Figure 6. (A,B,C) Relative average vertical swimming activity of all free-running animals: (A) homozygous for the wild-type copy of *PhBmal1* (+/+) (A); heterozygous for the mutant and wild-type alleles (B); and homozygous for the mutant allele (C). SEM and subjective day and night represented as in Figure 1 and 3. Individual animals who had periods of inactivity lasting >48 hours were removed to prevent skewing of the data. (D) Average

power of rhythmic animals does not significantly vary by genotype for vertical swimming (Kruskal-Wallis ANOVA, p = 0.8807). (E) The free-running roaming activity of a single rhythmic +/+ animal is shown. (F) The corresponding periodogram of the +/+ behavior is shown. (G) The free-running roaming activity of a single +/Δ individual is shown. (H) The corresponding periodogram of the +/Δ behavior is shown, also demonstrating three significant peaks. (I) The free-running roaming activity of a single Δ/Δindividual is shown. (J) The corresponding periodogram of the Δ/Δ individual.

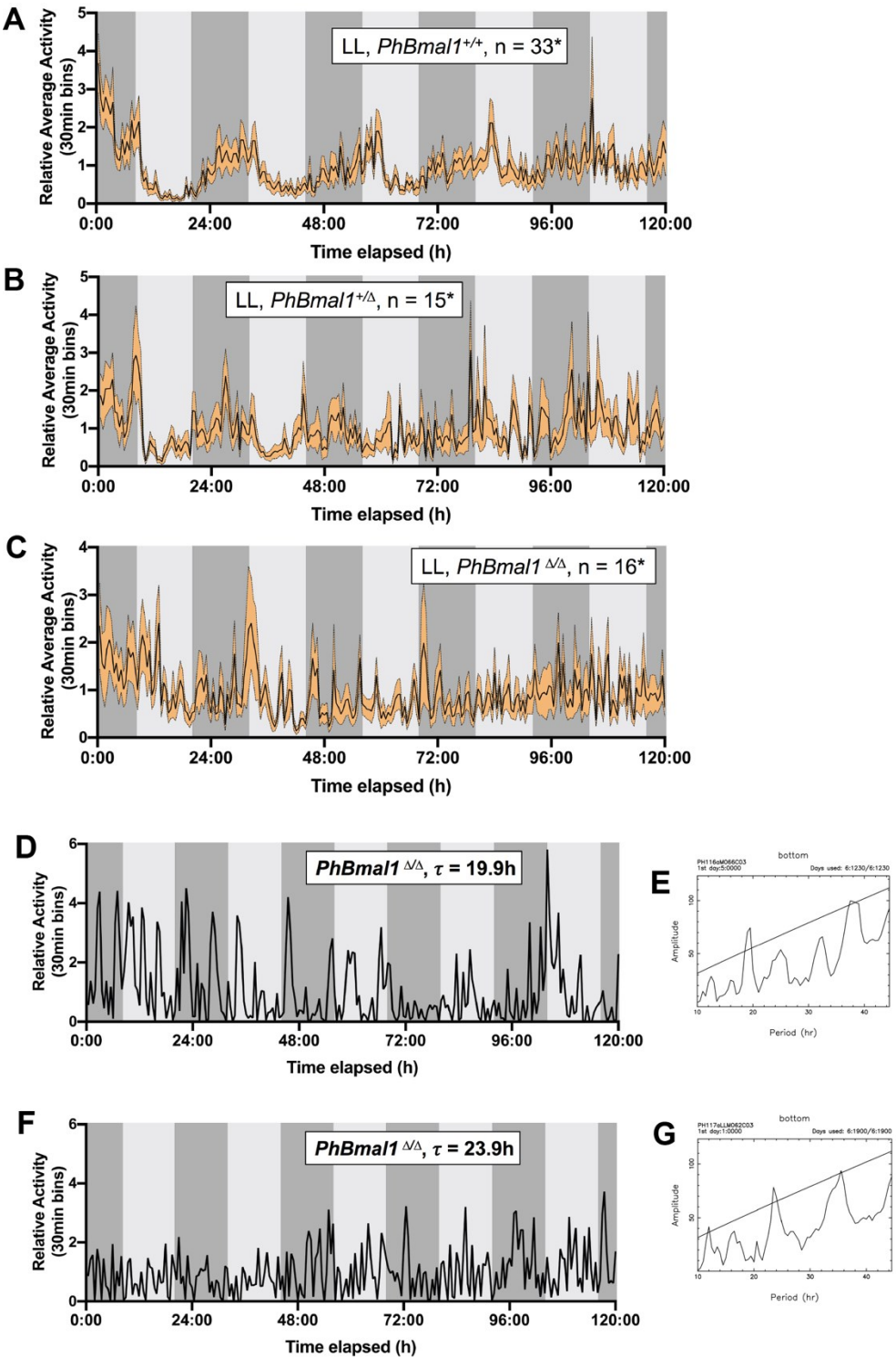

Figure S6. Loss of *PhBmal1* disrupts circadian rhythms in LL, related to Figure 6. (A,B,C) Relative average vertical swimming activity of all free-running animals: (A) homozygous for the wild-type copy of *PhBmal1* (+/+) (A); heterozygous for the mutant and wildtype alleles (B); and homozygous for the mutant allele (C). SEM and subjective

day and night represented as in Figure 1 and 3. Individual animals who had periods of inactivity lasting >48 hours were removed to prevent skewing of the data. Average power of rhythmic animals is not shown, since there were no Δ/Δ individuals with rhythmic vertical swimming traces. (D,F) The free-running roaming activity of two different Δ/Δ individuals are shown. (E,G) The corresponding periodograms of the Δ/Δ individuals.

Entrainment	Free-running conditions		Singlet period			Doublet period		
	Light	Temperature	Period (h)	SEM	n	Period (h)	SEM	n
LHT 13:20	DD	25ºC	12.43	0.04	35	24.68	0.09	36
LHT 13:20	LL	25ºC	12.47	0.05	21	24.79	0.13	23
LHT 19:20	DD	25ºC	12.50	0.04	33	24.89	0.12	31
LHT 19:20	LL	25ºC	12.45	0.05	21	24.78	0.07	24
LHT 13:20	LL	19.5ºC	12.58	0.10	21	24.60	0.20	22
LHT 13:20	LL	29ºC	12.28	0.06	16	24.50	0.16	17
12:12LD	DD	25ºC	12.16	0.09	7	24.35	0.12	16
12:12LD	LL	25ºC	12.00	0.60	2	25.64	0.35	25

Table S1. Free-running periods of male *Parhyale hawaiensis*, related to Figures 1 through 4. Entrainment was either to a tidal regimen (timing of last high tide [LHT] indicated), or 12:12LD-only regimen. Value “n” indicates the number of rhythmic animals with a singlet or doublet period.